

University of Windsor

Scholarship at UWindor

Electronic Theses and Dissertations

Theses, Dissertations, and Major Papers

2010

Model based control of exhaust gas recirculation valves and estimation of spring torque

Nazila Rajaei
University of Windsor

Follow this and additional works at: <https://scholar.uwindsor.ca/etd>

Recommended Citation

Rajaei, Nazila, "Model based control of exhaust gas recirculation valves and estimation of spring torque" (2010). *Electronic Theses and Dissertations*. 7866.
<https://scholar.uwindsor.ca/etd/7866>

This online database contains the full-text of PhD dissertations and Masters' theses of University of Windsor students from 1954 forward. These documents are made available for personal study and research purposes only, in accordance with the Canadian Copyright Act and the Creative Commons license—CC BY-NC-ND (Attribution, Non-Commercial, No Derivative Works). Under this license, works must always be attributed to the copyright holder (original author), cannot be used for any commercial purposes, and may not be altered. Any other use would require the permission of the copyright holder. Students may inquire about withdrawing their dissertation and/or thesis from this database. For additional inquiries, please contact the repository administrator via email (scholarship@uwindsor.ca) or by telephone at 519-253-3000ext. 3208.

Model Based Control of Exhaust Gas Recirculation Valves and Estimation of Spring Torque

By
Nazila Rajaei

A Thesis

Submitted to the Faculty of Graduate Studies
through the Department of Electrical and Computer
Engineering in Partial Fulfillment of the Requirements
for the Degree of Master of Applied Science at
The University of Windsor
Windsor, Ontario, Canada

2010

© 2010 Nazila Rajaei



Library and Archives
Canada

Published Heritage
Branch

395 Wellington Street
Ottawa ON K1A 0N4
Canada

Bibliothèque et
Archives Canada

Direction du
Patrimoine de l'édition

395, rue Wellington
Ottawa ON K1A 0N4
Canada

Your file *Votre référence*
ISBN: 978-0-494-62735-8
Our file *Notre référence*
ISBN: 978-0-494-62735-8

NOTICE:

The author has granted a non-exclusive license allowing Library and Archives Canada to reproduce, publish, archive, preserve, conserve, communicate to the public by telecommunication or on the Internet, loan, distribute and sell theses worldwide, for commercial or non-commercial purposes, in microform, paper, electronic and/or any other formats.

The author retains copyright ownership and moral rights in this thesis. Neither the thesis nor substantial extracts from it may be printed or otherwise reproduced without the author's permission.

In compliance with the Canadian Privacy Act some supporting forms may have been removed from this thesis.

While these forms may be included in the document page count, their removal does not represent any loss of content from the thesis.

AVIS:

L'auteur a accordé une licence non exclusive permettant à la Bibliothèque et Archives Canada de reproduire, publier, archiver, sauvegarder, conserver, transmettre au public par télécommunication ou par l'Internet, prêter, distribuer et vendre des thèses partout dans le monde, à des fins commerciales ou autres, sur support microforme, papier, électronique et/ou autres formats.

L'auteur conserve la propriété du droit d'auteur et des droits moraux qui protègent cette thèse. Ni la thèse ni des extraits substantiels de celle-ci ne doivent être imprimés ou autrement reproduits sans son autorisation.

Conformément à la loi canadienne sur la protection de la vie privée, quelques formulaires secondaires ont été enlevés de cette thèse.

Bien que ces formulaires aient inclus dans la pagination, il n'y aura aucun contenu manquant.

■+■
Canada

DECLARATION OF PREVIOUS PUBLICATION

This thesis includes 2 original papers that have been previously published/accepted for publication:

Thesis chapter	Paper title	Publication status
Chapter 4,5	“Model Predictive Control of Exhaust Gas Recirculation Valve”, 2010 SAE World Congress and Exhibition, Detroit, Michigan, USA.	Published
Chapter 4,6	“Spring Torque Estimation in an Electronic Throttle Valve”, IEEE VPPC Conference, 2010.	Accepted

I certify that I have obtained a written permission from the copyright owner(s) to include the above published material(s) in my thesis. I certify that the above material describes work completed during my registration as graduate student at the University of Windsor.

I declare that, to the best of my knowledge, my thesis does not infringe upon anyone's copyright nor violate any proprietary rights and that any ideas, techniques, quotations, or any other material from the work of other people included in my thesis, published or otherwise, are fully acknowledged in accordance with the standard referencing practices. Furthermore, to the extent that I have included copyrighted material that surpasses the bounds of fair dealing within the meaning of the Canada

Copyright Act, I certify that I have obtained a written permission from the copyright owner(s) to include such material(s) in my thesis.

I declare that this is a true copy of my thesis, including any final revisions, as approved by my thesis committee and the Graduate Studies office, and that this thesis has not been submitted for a higher degree to any other University or Institution.

ABSTRACT

Exhaust Gas Recirculation (EGR) valves have been used in diesel engine operation to reduce NOx emissions. In EGR valve operation, the amount of exhaust gas re-circulating back into the intake manifold is controlled through the open position of the valve plate to keep the combustion temperature lower for NOx emission reduction. Most of the control methods do not provide sufficient control accuracy on the valve position and the response time. Here, the model of a motor driven EGR valve is first identified through experiments and then the Generalized Predictive Control (GPC) method is applied to control the plate position of the valve. At the next step, to have a faster and more accurate control of the valve the torque generated by the spring connected inside the valve is estimated. The spring torque is considered as an external disturbance torque and three filters: Kalman, H_∞ and H_∞ Gaussian Filters are used to estimate this torque.

DEDICATION

I dedicate this thesis to:

my father whom I owe a lot,

and to all members of my family for their continuous love and support,

and to my mother who is always with us in spirit.

ACKNOWLEDGEMENTS

I would like to express my sincere appreciation to Dr. Xiang Chen and Dr. Ming Zheng, my co-supervisors, for their invaluable guidance and encouragement. They guided me throughout my thesis with great patience.

I would also like to express my gratitude to Dr. Behnam Shahrava and Dr. Jimi Tjong for their kindness assistance and valuable comments during the evaluation of this thesis and seminars.

I am very grateful to Mr. Frank Cicchello, Mr. Don Tersigni, Mr. Steve Budinsky, Mr. Dean Poublon and Mr. Andy Jenner, for their technical support throughout my research.

I am very grateful to the University of Windsor for the support of my graduate studies in these two years.

Finally, I thank my fellow graduate students, especially Ms. Smitha Cholakal, for their encouragement and continuous support during my stay at the University of Windsor.

TABLE OF CONTENTS

Declaration of Previous Publication.....	iii
Abstract.....	iv
Dedication.....	v
Acknowledgments.....	vi
List of Figures.....	ix
List of Tables.....	x

1. INTRODUCTION

1.1 Exhaust Gas Recirculation (EGR).....	1
1.2 Current Control Methods.....	2
1.3 Proposed Control Method.....	3
1.4 Estimation of Spring Torque	3
1.5 Thesis Outline.....	5

2. PRELIMINARY THEORY

2.1 Model Predictive Control (MPC).....	7
2.2 Generalized Predictive Control (GPC) Algorithm.....	10
2.3 Filter (Observer) Design.....	14

3. Hardware Setup

3.1 Hardware-in-Loop Configuration.....	19
3.2 Hardware-in-Loop Equipment.....	21

4. Modeling EGR Valve

4.1 Model of EGR Valve.....	28
4.2 Validation of Model Parameters	36

5. Control Design for EGR Valve and Experimental Validation

5.1 GPC Algorithm for Control of the EGR Valve	38
5.2 Experimental Validation.....	43

6. Estimation of Spring Torque

6.1 Spring Torque Estimation for EGR Valve	48
--	----

6.2 Experimental Validation.....	53
7. Conclusion and Future Work	
7.1 Conclusion	58
7.2 Future Work.....	60
References.....	61
Vita Auctoris.....	64

TABLE OF FIGURES

- Fig. 1.1 EGR Sweep Soot NOx
- Fig. 2.1 MPC control loop
- Fig. 3.1 Hardware setup to control the EGR valve
- Fig. 3.2 Hardware setup to estimate the spring torque
- Fig. 3.3 Block diagram of TMS320LF2407 EVM
- Fig. 3.4 Motion Mind driver
- Fig. 3.5 Dynamometer driver control inputs
- Fig. 4.1 The EGR valve and motor gearing to the plate shaft
- Fig. 4.2 The schematic diagram of the EGR valve
- Fig. 4.3 The block diagram of EGR valve
- Fig. 4.4 Plate speed response for the applied 10 V
- Fig. 4.5 Plate current response for the applied 10 V
- Fig. 5.1 The block diagram of the EGR valve controlled by GPC
- Fig. 5.2 EGR valve response for an 83.32 ° opening reference
- Fig. 5.3 Magnified view of EGR valve response for an 83.32 ° opening reference
- Fig. 5.4 EGR valve response for a 27.77° closing reference
- Fig. 5.5 Magnified view of EGR valve response for a 27.77° closing reference
- Fig. 5.6 Comparison of the responses of GPC and PID controller in opening direction
- Fig. 5.7 Comparison of the responses of GPC and PID controller in closing direction
- Fig. 5.8 EGR valve response for a sine reference
- Fig. 6.1 Observer model for spring torque estimation
- Fig. 6.2 Estimated spring torque result, Case 1
- Fig. 6.3 Spring torque estimation error, Case 1
- Fig. 6.4 Estimated spring torque, Case 2
- Fig. 6.5 Spring torque estimation error, Case 2
- Fig. 6.6 Estimated spring torque , Case 3
- Fig. 6.7 Spring torque estimation error, Case 3

LIST OF TABLES

Table 4.1 EGR valve identified parameters

Table 6.1 State space model of a general system and its model

CHAPTER 1

INTRODUCTION

1.1 Exhaust Gas Recirculation (EGR)

Exhaust Gas Recirculation (EGR) has been established as the most common methodology to reduce the oxides of nitrogen emission (NO_x) in diesel engines. It has also other effects on diesel engine combustion and exhaust emissions. Participation of carbon dioxide and water vapour particles in the combustion process, increase in the specific heat capacity of the engine inlet charge, and reduction of inlet charge mass flowrate are the other effects of exhaust gas recirculation in diesel engines. Exhaust gas recirculation valve re-circulates a portion of exhaust gas back into the intake manifolds which result in lower oxygen concentration and lower flame temperature. This results in reduced NO_x emission since the formation of this pieces becomes significant once the local temperature exceeds approximately 1800K [1-4].

A detailed analysis of EGR operation and its effects on emission and performance of diesels engines in different load conditions has been studied and can be found be found in literatures [5-7]. More over the EGR effects on emission control of spark ignition engines and dual fuel engines have been addressed as well [8-10].

Besides the direct effect on NO_x emission and temperature control of the engine, the EGR also has an indirect effect on soot emission. As can be seen in Fig. 1.1, when NO_x drops

below 0.5 g/kW-hr, soot increases significantly with a high rate of increase. This means a little EGR ratio increase will result in high soot emission.

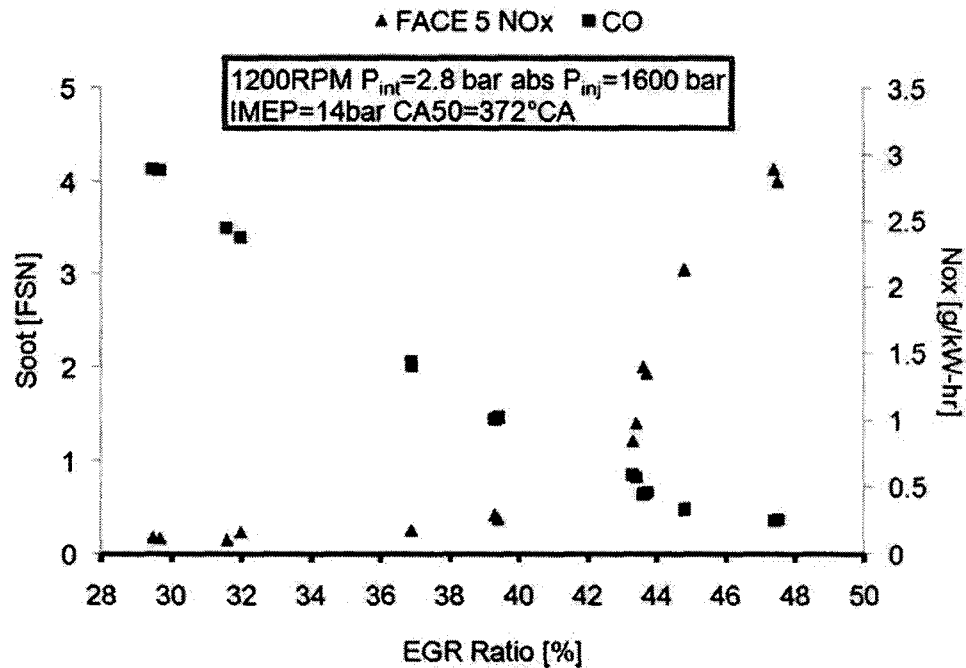


Fig. 1.1 EGR Sweep Soot NOx

The portion of exhaust gas re-circulated back into intake manifolds is controlled through to the open position of an EGR valve. So, an accurate and fast EGR valve control is necessary to meet modern emission standards.

1.2 Current Control Methods

Different approaches have been proposed to address the control of the valves in general. In [11-14] the methods to control the EGR valve are detailed. Usual implementations are based on PID algorithm. In [32] the control strategy based on neural networks is discussed. A discrete-time implementation of a variable structure controller with sliding mode observer is detailed in [33] and a cascade control scheme for a throttle body is

proposed in [34]. In [35] two simplified different sliding mode controllers based on a simplified second order plant model are presented.

However, these control methods which are currently in use, such as PID or sliding mode controller, take an enormous effort to find the optimized parameters for the controllers, and in many cases they cannot provide sufficient control accuracy on the valve position. In fact, in most cases, the designed system could not meet the required performances.

1.3 Proposed Control Method

The throttle valves are usually controlled in one direction, opening direction, using unidirectional drivers and closed automatically with the spring force. In advanced control techniques, the throttle valve is controlled in both opening and closing directions using a bidirectional driver. So, with an appropriate control method and using a bidirectional driver the valve could be precisely controlled in both closing and opening direction. Here the Model Predictive Control method is proposed to control the valve.

Model predictive control method does not yield the optimal solution for the control problem but with a good approximation at each instant calculates the control inputs using the receding horizon concept. In fact the purpose of this method is to drive the future outputs of the system close to the defined reference trajectory.

1.4 Estimation of Spring Torque

Electric throttle valves driven by DC motors have been used broadly in automotive engine control to improve engine performance so that emission standards could be

satisfied [25-27]. Specifically, low temperature combustion is a hopeful mode that would facilitate low NO_x emission while still keeping the engine efficiency high [25]. An important fact in such a mode is that the feasible combustion window is very narrow. This in general requires faster transient responses from controlling valves and, hence, calls for advanced control of valve operation that could allow faster and accurate performance. In the EGR valve case, the accuracy requirement for the valve plate position (opening or closing) would be more stringent and the control must be more prompting in order to facilitate low temperature combustion

The total torque acting on the valve plate is actually the sum of the motor torque and a spring torque which goes against the plate during opening session and serves as an extra assisting torque during the closing session. Since this spring torque is not regulated by the motor drive controller, for faster and more accurate control of such a throttle valve it is important to estimate the spring torque so that the information could be used to further improve the motor torque control. Here, the spring torque is treated as a disturbance torque and model based robust estimations are developed using the ideas in [22-24] to estimate this torque in a throttle valve.

The disturbance torque estimation for a DC motor is reviewed in many literatures. In [21-23], estimation of disturbance torque on the DC motor shaft has been proposed and developed. In [21] the disturbance torque acting on the motor shaft is assumed to be constant with respect to the dynamics of the filter and a Luenberger filter is proposed [21]. In [22-23], the disturbance torque is treated as an uncertain variable input and a developed robust filter [24] is applied to estimate the motor speed and current so that the

estimation of the disturbance torque could be calculated from the current and speed estimation.

Hence, to have a faster and more accurate control of the throttles valve which is a necessary in advanced control engine, the spring torque is treated as a disturbance torque applied to the motor shaft and three filter designs, namely, Kalman, H_∞ , and, H_∞ Gaussian, are developed and compared to estimate the spring torque

1.5 Thesis Outline

This thesis is arranged as follow: in Chapter 2 the preliminary theory of Model Predictive Control method and Generalized Predictive Control algorithm is detailed. The theory required for the observer design and different methods to calculate the observer gain are developed.

In Chapter 3 Hardware-in-Loop (HIL) setup configuration and tests done to evaluate the effectiveness of proposed control algorithm for the EGR valve are detailed, and the configuration and method to obtain the spring torque is presented.

In Chapter 4 the model of the EGR valve is derived. The model parameters are identified while the identification methods are discussed and the accuracy of the parameters are validated.

In Chapter 5 based on the model of the system and the parameters identified in Chapter 4, the GPC algorithm for the EGR valve is derived, the future output of the plant and the control input of the system are obtained and the experimental validations are shown.

In Chapter 6 using the model obtained in Chapter 4, the methodology to design the spring torque observer for the EGR valve which includes the state space models of observers is detailed. The experimental validations for the estimated torque are shown.

Finally the thesis is concluded in Chapter 7 and recommendations are made for future work in this area.

CHAPTER 2

PRELIMINARY THEORY

2.1 Model Predictive Control (MPC)

Model Predictive Control method (MPC) refers to a wide range of control methods which uses the model of the system to minimize a cost function and consequently to calculate the control signal [15]. This wide range of MPC methods is only different in the defined system model, the cost function and the noises [15]. In this method a sequence of future outputs is predicted using the process model, while the control sequence is calculated by minimizing an objective function [15]. This objective function is defined in terms of system error between the predicted output and reference trajectory [15]. The advantage of this method is to the use of predictive inputs sequence which would allow a faster control on the system. For this purpose to reflect the full dynamics of the system, it is necessary to model the plant in the best possible way.

The methodology of all the controllers belong to MPC family is represented in [15]. This method applies a dynamic model of the plant to generate a set of predicted outputs $\hat{y}(t + j|t)$ in a finite horizon, N sampling time, by using the known input and output values up to the present time. At the same time the criteria function, usually defined in terms of error signal between the predicted output and the defined reference trajectory, is minimized during the process and the set of future control signals is calculated. Since at each sampling time all the sequences are brought up to date only the first element $u(t|t)$

of the control sequence, the signal corresponding to the time t , is sent to the system and the new data is used to calculate the next control signal $u(t+1|t+1)$.

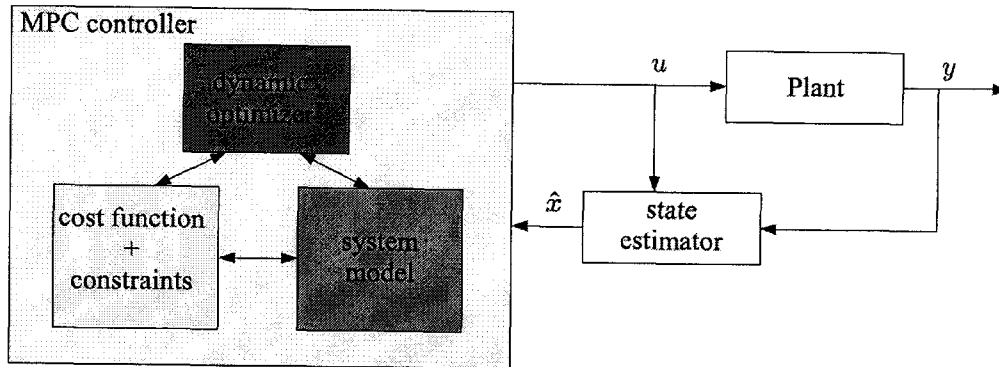


Fig. 2.1. MPC control loop

The basic structure to implement the MPC strategy is shown in Fig. 2.1. As can be seen, using the plant model the future output of the system is predicted based on the past input and output of the system and the optimized future outputs. These predicted output are compared with the defined reference trajectory, and the error comes from the difference of these two signals is minimized and used to calculate the next control input by the optimizer [15-17].

Therefore, this approach provides a forward prediction in the control and hence can potentially provide a faster response while the accuracy can be improved during the operating process in the long-run.

The model predictive control method consists of three main elements of:

1. Predictive Model
2. Objective Function
3. Obtaining the control law

According to the different options which can be used for each of these elements the proposed algorithm may vary [15].

1. Predictive Model

Since this method is a model based method, the process model plays a critical role in the controller. The plant model should be able to fully capture the system dynamics, while it should be simple enough to implement, and allow the prediction of the future outputs to be calculated and analyzed [15]. Various types of models are used in different MPC formulations. Impulse response, step response, state space, transfer function and nonlinear models are different methods which could be used in the MPC formulation according to the chosen method. Selection of disturbances model, the difference between the measured output and the one calculated by the model, is also as critical as choosing an appropriate process model [15].

2. Objective Function

Various MPC algorithms may use different objective functions to calculate the control law. The purpose of defining this criterion is that the predicted output follows a defined reference trajectory, minimizing the future error, on a finite control horizon, while the future control signals applied to the system are calculated. The most common expression for this function takes the quadratic form of the errors between the predicted future outputs and the defined reference trajectory.

3. Obtaining the Control Law

The control signal sent to the system is calculated by minimizing the objective function on a finite control horizon. So this signal is a function of the past inputs and outputs of the system which are known at the present sampling time and the predicted future outputs and the reference trajectory defined for the system.

2.2 Generalized Predictive Control Algorithm

Generalized Predictive Control (GPC) is one of the most popular Model Predictive Control (MPC) methods proposed by Clarke al. [16-17]. This method is capable of controlling a wide range of plants with variable design parameters and variable dead-time, and even unstable and non-minimum phase plant [15-17]. It is a proven successful control strategy for industrial application as long as the sampling period implemented is long enough to carry out the calculation [18]. This control method has been used in applications such as autopilot design [18], brushless DC drives [19], and direct drives [20].

GPC method is based on the same concept as MPC and has many ideas in common with the other predictive controllers, but it has some differences as well [15]. This method can deal with unstable and non-minimum phase plant and incorporates the concept of control horizon as well as the consideration of weighting of control increments in the cost function [15].

A single-input-single-output (SISO) plant, when linearized and regulated around a particular set point can be modeled by a Controller Controlled Auto-Regressive and Integrated Moving Average (CARIMA) model [15-17]:

$$A(z^{-1})y(t) = B(z^{-1})u(t-1) + \frac{C(z^{-1})\zeta(t)}{\Delta} \quad (2.1)$$

Where $u(t)$ and $y(t)$ are the control and output sequence of the system, $\zeta(t)$ is the zero mean white noise, and Δ is the differencing operator $1 - z^{-1}$. A, B and C are polynomials in the backward shift operator z^{-1} :

$$\begin{aligned} A(z^{-1}) &= 1 + a_1z^{-1} + a_2z^{-2} + \dots + a_{na}z^{-na} \\ B(z^{-1}) &= b_0 + b_1z^{-1} + b_2z^{-2} + \dots + b_{nb}z^{-nb} \\ C(z^{-1}) &= 1 + c_1z^{-1} + c_2z^{-2} + \dots + c_{nc}z^{-nc} \end{aligned} \quad (2.2)$$

For simplicity, the C polynomial is chosen to be 1 or C^{-1} is truncated and absorbed into A and B [15-17].

The GPC controller specifications are formally described using the following cost function [15]:

$$J(N_1, N_2, N_u) = \sum_{j=N_1}^{N_2} \delta(j)[y(t+j|t) - w(t+j)]^2 + \sum_{j=1}^{N_u} \lambda(j)[\Delta u(t+j-1)]^2 \quad (2.3)$$

Where N_1 , N_2 are the minimum and maximum costing horizons, N_u is the control horizon. In the systems with unknown dead-time N_1 can be to 1 with no loss of stability, and in discrete time event N_2 should exceed the degree of $B(z^{-1})$. N_u is an important control parameter. For a simple system even a value of 1 gives acceptable control. The

value of N_u could increase till it reaches the stage that any further increase in this parameter makes very little difference [15-17]. $\delta(j)$, and $\lambda(j)$ are the weighting factors of the predicted error and the control effort during the optimization [15-17]. In the above equation, in the most cases a reference trajectory $w(t+j)$ is used which does not necessarily have to coincide with the real reference. It is usually a first order approximation of the current output values towards the known reference [15]

$$w(t) = y(t) \quad w(t+k) = \alpha w(t+k-1) + (1-\alpha)r(t+k) \quad k=1..N \quad (2.4)$$

Where α is a parameter between 0 and 1. By choosing a small value of α a fast tracking of the reference is provided while increasing this parameter yields a smooth reference tracking.

The next Diophantine equation is used to calculate the future output sequence:

$$1 = E_j(z^{-1})\tilde{A}(z^{-1}) + z^{-j}F_j(z^{-1}) \quad (2.5)$$

Where: $\tilde{A}(z^{-1}) = 1 - A(z^{-1})$

The E_j and F_j polynomials can be obtained by dividing 1 over the $\tilde{A}(z^{-1})$ to the point that the remainder can be factorized as $z^{-j}F_j(z^{-1})$ [15-17].

If the multiplication of the CARIMA equation with $\Delta E_j(z^{-1})z^j$ is substituted into the Diophantine equation the j th step ahead sequence of the output plant can be obtained.

After the mathematical calculation the future output of the plant can be obtained by:

$$y = Gu + F(z^{-1})y(t) + G'(z^{-1})\Delta u(t-1) \quad (2.6)$$

Where:

$$y = \begin{bmatrix} \hat{y}(t+1|t) \\ \hat{y}(t+2|t) \\ \vdots \\ \hat{y}(t+N|t) \end{bmatrix} \quad u = \begin{bmatrix} \Delta u(t) \\ \Delta u(t+1) \\ \vdots \\ \Delta u(t+N) \end{bmatrix}$$

$$G(z^{-1}) = E(z^{-1})B(z^{-1}) = \begin{bmatrix} g_0 & 0 & \cdots & 0 \\ g_1 & g_0 & \cdots & 0 \\ \vdots & \vdots & \vdots & \vdots \\ g_{N-1} & g_{N-2} & \cdots & g_0 \end{bmatrix} \quad F(z^{-1}) = \begin{bmatrix} F_1(z^{-1}) \\ F_2(z^{-1}) \\ \vdots \\ F_N(z^{-1}) \end{bmatrix}$$

$$G'(z^{-1}) = \begin{bmatrix} (G_{d+1}(z^{-1}) - g_0)z \\ (G_{d+2}(z^{-1}) - g_0 - g_1z^{-1})z^2 \\ \vdots \\ (G_{d+3}(z^{-1}) - g_0 - g_1z^{-1} - \cdots - g_{N-1}z^{-(N-1)})z^N \end{bmatrix}$$

The last two terms of the above equation clarify the past information of the plant and can be grouped as f .

Therefore, the future output equation can be written as:

$$y = Gu + f \quad (2.7)$$

Finally, the future control input can be obtained by minimizing the cost function over the control horizon. By considering the two weighting factors λ and δ in minimization the control input is calculated. Equation (2.3) can be written as:

$$J = \delta \times (Gu + f - w)^T (Gu + f - w) + \lambda u^T u \quad (2.8)$$

After simplification, the objective function is written as:

$$J = \frac{1}{2}u^T H u + b^T u + f_0 \quad (2.9)$$

where:

$$\begin{aligned} H &= 2(\delta G^T G + \lambda I) \\ b^T &= 2\delta(f - w)^T G \\ f_0 &= \delta(f - w)^T (f - w) \end{aligned} \quad (2.10)$$

By making the gradient of J equal to zero, the minimum of J is obtained:

$$u = -H^{-1}b = (\delta G^T G + \lambda I)^{-1} \delta G^T (w - f) \quad (2.11)$$

The control signal sent to the plant is the first element of the vector u which is given by:

$$\Delta u(t) = K(w - f) \quad (2.12)$$

Where K is the first row of matrix $(\delta G^T G + \lambda I)^{-1} \delta G^T$ and w is the defined reference trajectory.

2.3 Filter (Observer) Design

For an ideal system where no disturbance and model uncertainty is considered on the system, the Luenberger filter is used as the simplest filter design. In fact, Luenberger filter is designed for an ideal system, and its performance in the real world is usually not satisfactory. So, here the performance of three robust filters is developed to estimate the

spring torque as an external disturbance torque while considering the model uncertainty and disturbances on the system.

- ***Kalman Filter***

Kalman filter is used to estimate the state variables for the system subjected to the white noise. This filter estimates the state variables in a noisy environment by minimizing the variance of the estimation error.

For Kalman filter design, the state space model of the valve system is modified by including noises in:

$$\begin{aligned}\dot{x} &= Ax + Bu + \zeta \\ z &= C_1x \\ y &= C_2x + \theta\end{aligned}\tag{2.13}$$

Here x is the state variable, u is system input, y is the measured output, z is the desired output, A and B depend on the model parameters.

In the state space model of Kalman filter, ζ and θ are the noise inside the valve system and in the measurement respectively. It is assumed that the average values of both the noises, ζ and θ , are zero and there is no correlation between them. These two noises are modeled by a white noise w_0 with power spectrums: $\zeta = B_0w_0$ and $\theta = D_{20}w_0$. In practice, B_0 and D_{20} are set by measuring the covariance of the measurement noise and process noise respectively.

The filter gain is obtained by solving the Riccati equation [28, 29 and 30]:

$$(A - B_0 D_{20}^T R_0^{-1} C_2)P + P(A - B_0 D_{20}^T R_0^{-1} C_2)^T + B_0(I - D_{20}^T R_0^{-1} D_{20})B_0^T - PC_2^T R_0^{-1} C_2 P = 0 \quad (2.14)$$

So:

$$L_k = -(B_0 D_{20}^T + PC_2)R_0^{-1} \quad (2.15)$$

where: $R_0 = D_{20} D_{20}^T$

- **H_∞ Filter**

When the system model parameters are uncertain and bound to change with time or process, these uncertainty should be taken into account when the state variables are estimated. For such a system, H_∞ filter is designed to make the state estimation robust to changes in model parameters.

$$\begin{aligned} \dot{x} &= Ax + Bu + B_1 w \\ z &= C_1 x \\ y &= C_2 x \end{aligned} \quad (2.16)$$

B_1 is the weight given to the uncertainty disturbances, w , depending on its effect on the system performance.

The H_∞ filter gain is obtained by solving the Riccati equation [31]:

$$AP + PA^T + P(\gamma^{-2} C_1^T C_1 - C_2^T C_2)P + B_1 B_1^T = 0 \quad (2.17)$$

So:

$$L = -PC_2^T \quad (2.18)$$

Here γ is the design parameter which decides the limit of uncertainty which could be tolerated by the filter for good performance. Lower the value of γ , higher the tolerance of the filter towards to model uncertainty.

- *H_∞ Gaussian Filter*

A practical system is subjected to both white noise and parameter uncertainty. The Kalman filter is designed to achieve good performance against white noises while it is model dependant and sensitive to parameters variations. The H_∞ filter is designed to handle model parameters variation; however it does not to give good performance against white noise. So the performance of these two filters conflict each other. So for the case when the system is subjected to both model parameters uncertainty and white noise, H_∞ Gaussian filter is designed based on constrained optimization result and H_∞ optimization design. This filter is designed using a parameter γ which decides the weight which gives the weight that is given to the performance of each type of the filters, thus obtains a suitable balance between the performances of the two filters.

The system model that accommodates the H_∞ Gaussian filter is design by considering both white noises and model parameters uncertainty:

$$\begin{aligned} \dot{x} &= Ax + Bu + B_0w_0 + B_1w, \\ z &= C_1x, \\ y &= C_2x + D_{20}w_0, \end{aligned} \tag{2.19}$$

where w_0 , w , B_0 , and B_1 were introduced in part 1 and 2.

For the H_∞ Gaussian filter design, the filter gain is obtained through solving two Riccati equations [29]:

$$(A - P_2 C_2^T R_0^{-1} C_2 - B_0 D_{20}^T R_0^{-1} C_2)^T P_1 + P_1 (A - P_2 C_2^T R_0^{-1} C_2 - B_0 D_{20}^T R_0^{-1} C_2) + \gamma^{-2} P_1 B_1 B_1^T P_1 + C_1^T C_1 = 0 \quad (2.20)$$

$$(A - B_0 D_{20}^T R_0^{-1} C_2 + \gamma^{-2} B_1 B_1^T P_1) P_2 + P_2 (A - B_0 D_{20}^T R_0^{-1} C_2 + \gamma^{-2} B_1 B_1^T P_1)^T - P_2 C_2^T R_0^{-1} C_2 P_2 + B_0 (I - D_{20}^T R_0^{-1} D_{20}) B_0^T = 0 \quad (2.21)$$

So the gain value is calculated as:

$$L_{H_\infty G} = -(P C_2^T + B_0 D_{20}^T) R_0^{-1} \quad (2.22)$$

CHAPTER 3

Hardware Setup

3.1 Hardware-in-Loop Configuration

Hardware-in-Loop (HIL) testing is used to check the performance of a system design subject to real world loads and disturbances. In HIL simulation, only the designed system is composed of hardware parts, the remaining plant dynamics are provided by software. This testing helps in obtaining the required data before implementing the designed model in an actual system thus saving cost and time taken to test the efficiency of the design. It is also suitable in cases where testing the design in the entire system is not feasible due to physical constraints and safety reasons. The HIL setup to test the EGR valve control loop is shown in Fig. 3.1 and the setup to estimate the spring torque is shown in Fig. 3.2.

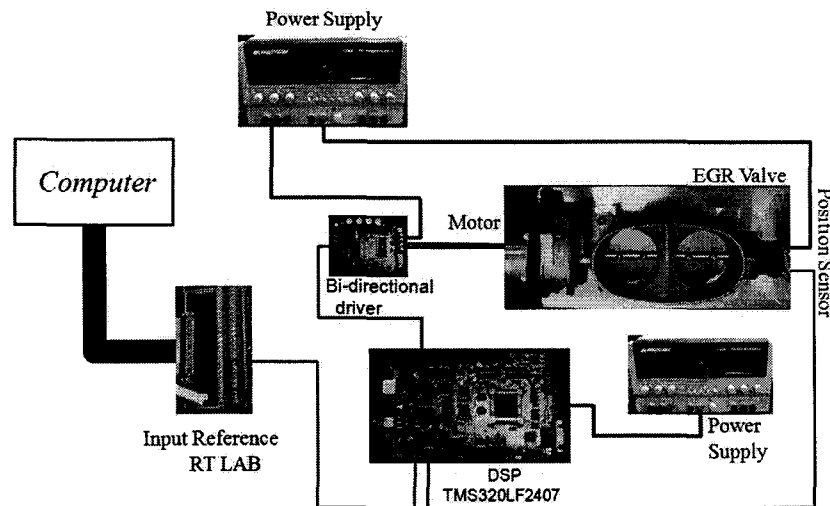


Fig. 3.1 Hardware setup to control the EGR valve

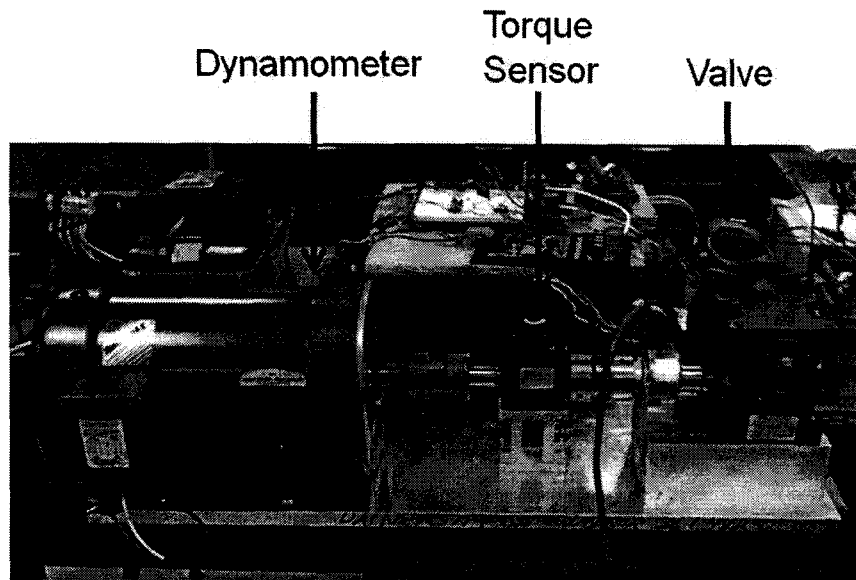


Fig. 3.2 Hardware setup to estimate the spring torque

In the hardware setup to control the EGR valve, Fig. 3.1, the GPC controller is implemented by a TMS320LF2407 DSP with 40MHz CPU clock. The reference voltage from the Opal-RT output terminal and the feedback voltage which in fact shows the plate angular position are the analog inputs of the DSP. The feedback voltage varies between around 1.4V for the fully close condition to 3.2V for the case when the valve is completely open. After applying the GPC algorithm, the output of the DSP is applied to a bidirectional driver in form of a PWM wave. This driver applies the control input as a voltage across the motor armature.

The experiment setup to measure the spring torque is shown in Fig. 3.2. As can be seen, the valve is connected to a dynamometer through a torque sensor. The torque sensor measures the effective torque acting on its shaft. In the experiment, the dynamometer produces a torque of 0.5 N.m applied to one end of the torque sensor shaft, on the other end is the valve torque magnified through the gear box. Since the torque sensor measures

the total torque on its shaft including the spring torque, it is impossible to obtain the spring torque through direct measurement. Therefore, an indirect way is conducted by performing two sets of experiments in order to calculate the spring torque. In the first experiment the spring is connected between the motor and the plate shaft. In this case the total torque acting on the torque sensor shaft is $T_{ts} = T_{dyno} + T_p - T_s$, where T_{ts} is the torque measured by the torque sensor, T_{dyno} is the dynamometer torque, T_p and T_s are the plate (hence the valve motor) and the spring torque respectively. In the second experiment the spring is taken off so the torque measured by the torque sensor is $T_{ts} = T_{dyno} + T_p$. Clearly, the difference in the two readings of the torque sensor would be the spring torque. During the experiments, the filter estimation is executed at the same real time as the real experiment to keep the integrity of the transient process. The experiment is done by applying voltage of $6V$ to the valve when the spring is disconnected and $4V$ to it when there is the spring connected there. These two voltages produce the same current and as a result the same motor torque. However, in the first case the valve opens completely and in the second case it opens only half way. Then the real valve operation (opening) and the filter estimation are conducted at the same time.

3.2 Hardware-in-Loop Equipment

- ***DSP TMS320LF2407***

The TMS320LF240x devices are part of the TMS320C2000 platform of fixed-point DSPs. The 240x devices offer the enhanced TMS320DSP architectural design of the C2xx core CPU for low-cost, low-power, and high performance processing capabilities.

Highly developed peripherals, optimized for digital motor and motion control applications, have been integrated to provide a single-chip DSP controller.

The 240x offers increased processing performance, 30M instruction per second, and a higher level of peripheral integration. It offers up 32K words of on chip Flash devices contain of 256-word boot ROM to facilitate in-circuit programming. It offers two event manager optimized for digital motor controller and power conversion applications. These two modules have the capability of controlling multiple motors and/or converters, generating symmetric and asymmetric PWM outputs, programmable dead band, and synchronized analog-digital conversion.

The following DSP peripherals are used in the EGR valve control development:

1. Analog to Digital (ADC) Converter Module

The ADC module consists of a 10-bit ADC with a built-in sample-and-hold (S/H) circuit. The high-performance, 10-bit analog-to-digital converter has a minimum conversion time of 500 ns. For these converters a maximum of 16 conversions is allowed to take place in a single conversion session without any CPU overhead.

2. Event-Manager Modules

The event-manager modules include general-purpose (GP) timers, full-compare/PWM units, and capture units. Only one of the two general-purpose timers is used to generate the desired PWM signal. This timer includes a 16-bit timer, up-/down-counter, TxCNT, a 16-bit timer-compare register, TxCMPR, a 16-bit timer-period register, TxPR, and a 16-bit timer-control register, TxCON. The period register shows the full period of the PWM signal, while the compare register indicates the time the signal is off.

The TMS320LF2407 evaluation module is used to apply the certain characteristics of the LF2407 DSP. Fig. 3.3 shows the basic configuration for LF2407 EVM and its features.

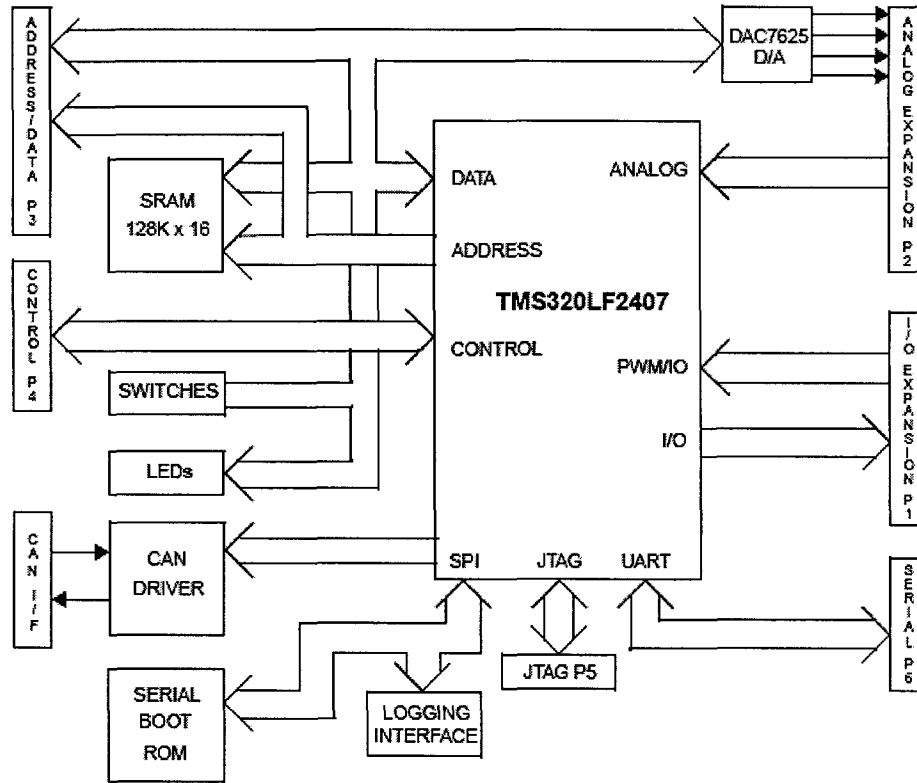


Fig. 3.3 Block diagram of TMS320LF2407 EVM

Two of 16 channels of analog to digital converter are used to convert the analog reference signal comes from the Opal-RT, and the system feedback comes from the position sensor to digital values. Using these two digital values the GPC control algorithm is implemented, and the control value is calculated. Since the control signal applied to the driver should be a PWM wave, this value is used to generate a PWM signal. The board is powered by a 5V analog voltage and grounded to the common ground of the DSP.

- **Motor Driver Configuration**

A PWM controlled driver board is used for bi-directional control of the DC motor connected to the EGR valve. The control signal from the DSP is applied to the driver control pins, J4 in Fig. 3.4, and the equivalent voltage is applied to the valve motor through pins 2 and 3 of J3. All connectors of the motor driver used in this development are shown in Fig. 3.4.

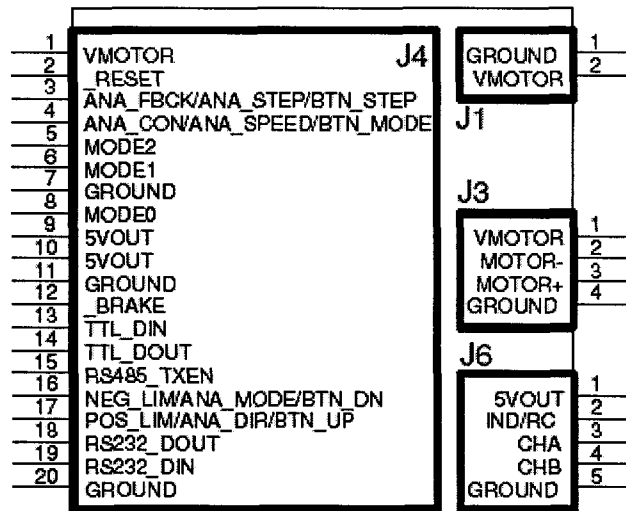


Fig. 3.4 Motion Mind driver

There are different operating modes for the driver. Here the bi-directional analog mode is used to control the valve in both directions. In this mode the 0-5V signal present at *ANA_SPEED* (J4 P4) is translated into the motor speed while a dead-band centered at 2.5V exists (2.43V-2.57V). If the analog input falls within this range then the motor is stopped. The relationship between the analog input to the driver board and its output is:

$$V_{out} = 2V_{in} - 5 \quad (3.1)$$

where V_{in} is the control signal sent by the DSP and V_{out} is the voltage applied to the motor.

- ***Dynamometer***

A 5hp, 3 phase, 240V, 22Amp Baldor induction motor is used as the dynamometer. This dynamometer produces a torque of 0.5 N.m on the torque sensor shaft. The maximum torque the motor can produce is 20.18 N.m and the minimum torque is 0.1 N.m.

- ***Dynamometer Controller Configuration***

A vector drive is used to control the torque of the dynamometer. The configuration used by the dynamometer is as follow:

Operating Mode: Bipolar, Open loop vector mode

Operating zone: Quiet variable torque, 8kHz PWM

Command source: Analog Input 2

Analog Input 1: Current limit source, 0 to 10V

Analog Input 2: Torque signal, -10V to 10V

The drive control is operated by the opto-isolated digital inputs J2-8 to J2-20 shown in Fig. 3.5. The opto inputs can be switches or logic signals. In this case transistors were used to switch the inputs on and off, as they can be controlled by analog signal from *Opal-RT*.

The torque produced by the dynamometer is controlled by Analog Input 2 and the direction is controlled by the digital switches FWD and REV. For a positive torque, a +ve signal is sent through Analog 2 and the direction is selected as FWD. For negative torque,

a $-ve$ signal is sent through Analog 2 and the REV direction is selected. The relationship between the control signal, V sent to the dynamometer and the torque, T (in Nm) is:

$$T = 3.6V + 0.036 \quad (3.2)$$

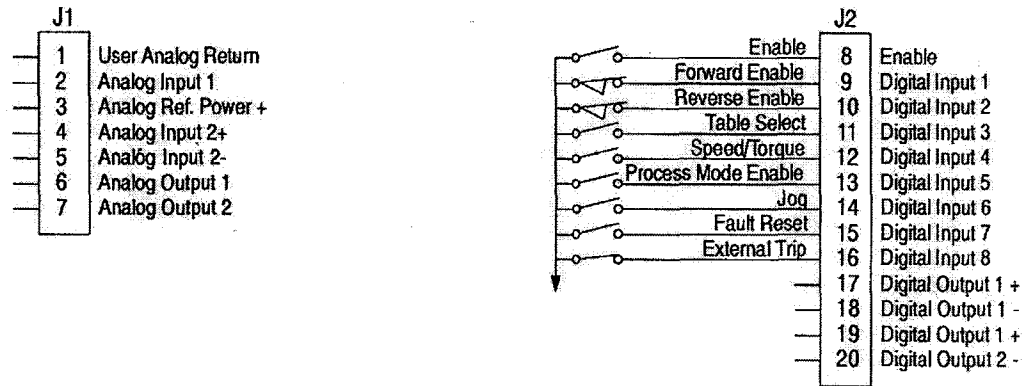


Fig. 3.5 Dynamometer driver control inputs

- **Gear Box**

Since it is expected that the spring torque be estimated as a very small value, a gearbox is used to amplify the valve (DC motor) torque. The ratio of the gear box is 1:20 which means the valve torque is magnified 20 times. The gearbox is designed such that the torque flow is permitted in only one direction from the high speed (low torque-input) side to low speed (high torque-output) side. This design is for safety reasons to ensure that the load does not drive the input under any direction.

- ***Torque Sensor***

A torque sensor is used to validate the estimation result of the spring torque. The torque sensor operated as any other strain gage sensor. When the motor is operated with no load torque acting on the gear box shaft, dynamometer in off condition, the output of the sensor is zero as there is no torsion force on the torque sensor shaft. When the dynamometer is in on condition, the torque sensor shows sum of the total torque acting on its shaft.

- ***Opal-RT Configuration***

The Opal-RT is configured to run a 1ms step size and the data is stored by using the *Opwrite* data logging block. Opal-RT is used in both the development to control the EGR valve and to estimate the spring torque. In the first development, since the control algorithm is implemented by the DSP the Opal-RT is only used to apply the reference signal, plot and store the control results. In the second development, the Opal-RT is used to get the current and voltage samples of the system and run the observer model at the same real time as the real experiment.

CHAPTER 4

Modeling EGR Valve

4.1 Modeling of EGR Valve

The electric throttle valve modeled in this study is a two plate butterfly valve driven with a low power DC motor. The DC motor mounted on top of the plate body is connected to the plate shaft through the gears. So the motor torque is magnified through these gears when applied on the plate shaft. The other side of the plate shaft is connected to a position sensor. This sensor is in fact a potentiometer converts the plate angular position into a DC voltage used for the plate position control. This output voltage varies in the range from 1.4 *V* to 3.2 *V*. The voltage 1.4 *V* shows the valve fully close position and 3.2 *V* shows the fully open position of the EGR valve.

Also there is a spring connects the plate shaft to the motor shaft. This spring adds an extra torque to the plate which helps the valve in closing direction and acts against it in opening movement. In Fig. 4.1 the EGR valve modeled in this study and the motor gearing part to the plate shaft is shown.

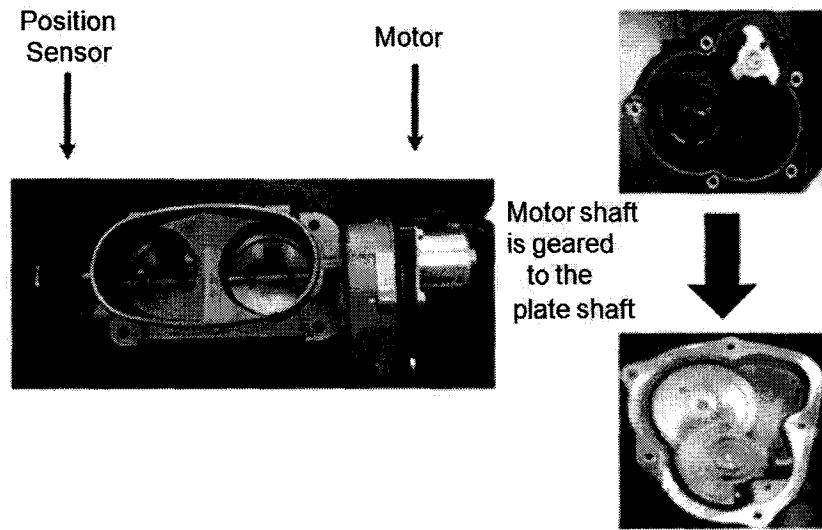


Fig. 4.1 The EGR valve and motor gearing to the plate shaft

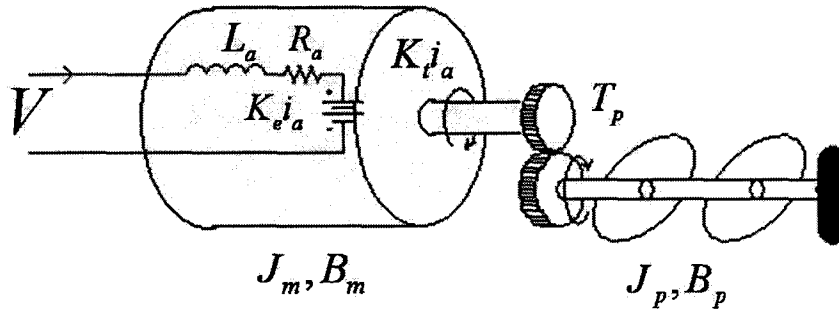


Fig. 4.2 The schematic diagram of the EGR valve

In order to model the EGR valve, first the DC motor which drives the valve is modeled, and its state space model is derived. The plate connected to the motor is treated as an

additional torque added on the motor shaft. So the full model of the valve could be derived.

The armature controlled DC motor provides the motor torque to drive the plates. It is noted that the motor torque is amplified through the gearbox before applying the plate shaft. The following equations can be established to model the motor drive.

$$V = R_a i_a + L_a \frac{di_a}{dt} + e_a \quad (4.1)$$

$$e_a = K_e \dot{\theta}_m \quad (4.2)$$

$$T_m = K_t i_a \quad (4.3)$$

$$T_m - T_f = J_m \ddot{\theta}_m + D_m \dot{\theta}_m \quad (4.4)$$

The electrical model of the motor is shown in equation (4.1) where R_a and L_a are resistance and inductance of the motor armature winding, i_a is the armature current, and e_a is the internally generated voltage which is proportional to the motor velocity. θ_m is the motor angular position. K_e and K_t are the voltage and torque constants which in SI units have the same value. In equation (4.4) the motor dynamic parameters, inertia and viscous damping factor, are denoted as J_m and B_m , while T_f is the friction torque on the motor.

The torque equation for the whole EGR system is shown in the following equation:

$$T_p = \bar{J} \ddot{\theta}_p + \bar{B} \dot{\theta}_p + nk_s \theta_p \quad (4.5)$$

where: $\bar{J} = J_p + n^2 J_m$, $\bar{B} = B_p + n^2 B_m$

Where \bar{J} and \bar{B} are the total moment of inertia and viscous damping factor of the system in which both motor and plate dynamic parameters are considered, n is the gear ratio and $nk_s\theta_p$ presents the stiffness of the spring which is actually ignored in the control design.

With equations (4.1) to (4.5), the electric throttle valve can be modeled in single shaft as follow:

$$V = R_a i_a + L_a \frac{di_a}{dt} + K_e n \dot{\theta}_p \quad (4.6)$$

$$T_m = K_t i_a \quad (4.7)$$

$$T_p = \bar{J} \ddot{\theta}_p + \bar{B} \dot{\theta}_p \quad (4.8)$$

The model derived above can be presented using Laplace transfer function in the block diagram shown in Fig. 4.3:

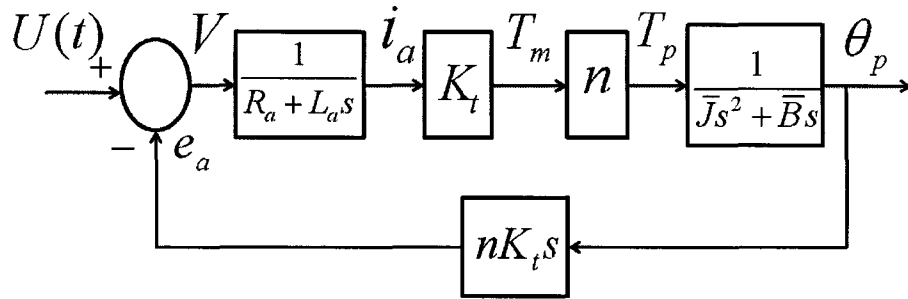


Fig. 4.3 The block diagram of EGR valve

In this block diagram T_m is the motor torque produced by the armature current. This torque after magnifying through gears drives the valve. The plate position is the output of this plant.

The state space model of the EGR system can be derived by considering armature current, plate angular position and plate angular speed as three states of the plant:

$$\begin{aligned} \dot{x} &= Ax + Bu \\ y &= Cx \end{aligned} \quad (4.9)$$

$$x = \begin{bmatrix} x_1 \\ x_2 \\ x_3 \end{bmatrix} = \begin{bmatrix} i_a \\ \theta_p \\ \dot{\theta}_p \end{bmatrix}, \quad u = V, \quad y = \theta_p$$

Using the system model the A, B and C are derived as:

$$A = \begin{bmatrix} \frac{-R}{L_a} & 0 & \frac{-K_t}{nL_a} \\ 0 & 0 & 1 \\ \frac{K_t}{\bar{J}} & 0 & \frac{\bar{B}}{\bar{J}} \end{bmatrix}, \quad B = \begin{bmatrix} \frac{1}{L_a} \\ 0 \\ 0 \end{bmatrix}, \quad C = [0 \ 1 \ 0]$$

In order to complete the model of the EGR valve the system parameters such as R_a , L_a , \bar{J} , \bar{B} , K_t should be identified. Since the system parameters for this development are not available, it is required to determine these values experimentally to obtain the complete EGR valve model. In order to determine the motor parameters R_a , L_a and K_t the experiments are conducted on the motor itself when it is disconnected from the plate. Two mechanical parameters \bar{J} and \bar{B} are obtained through the experiments on the whole valve.

1. Armature Resistance

A very small voltage, V_t , is applied to the motor terminals, the rotor is blocked for few seconds. Using a very small resistance, r_{shunt} , the current, i_a , is read quickly when it reaches the steady state. Since the rotor may heat up slightly it should not be blocked for a long time. The armature resistance can be calculated as:

$$R_a = \frac{V_t - r_{shunt} i_a}{r_{shunt}} \quad (4.10)$$

Since the armature resistance highly depends on the shaft position, the experiment is conducted several times on the motor and the final value is obtained by taking the average of the calculated values.

2. Armature Inductance

The armature inductance, L_a , could be calculated by measuring the phase lag between the motor low amplitude voltage and current when the motor rotor is blocked. Since the result of this experiment is too noisy in this case, the motor inductance is simply measured by using an inductance meter.

3. Electrical and Mechanical Constants

In a DC motor considering the SI units the electrical constant, K_v (V/rad/s) is equal to the mechanical constant, K_t (Nm/A). In this case the motor internally generated voltage is measured and used to calculate these two constants. For this experiment the valve is opened by hand and closed automatically when it connects to the motor. The motor

constants are calculated by measuring the voltage internally generated across the motor terminals, motor speed and the gear ratio.

So the motor constants are measured as follow:

$$K_v = K_t = \frac{v}{\omega_m} \quad (4.11)$$

where v is the motor internally generated voltage, ω_m is the motor speed in RPM.

4. System Viscous Damping Factor and Inertia

Since the system is modeled using the total viscous damping factor and total inertia, these two parameters are calculated by conducting couple of experiments on the whole valve.

In order to find system moment of inertia and viscous damping factor, 8 different step voltages in the range of 2-10V are applied to the EGR valve and the corresponding speed and current responses are analyzed. Fig. 4.4 shows the speed response of the system when a voltage of 10 V is applied to the system. The acceleration period is divided into 6 small periods; the system acceleration, speed and current are measured in these small periods and used to calculate the system inertia and damping factor.

$$K_v \times \begin{bmatrix} i_{a1} \\ i_{a2} \\ i_{a3} \\ i_{a4} \\ i_{a5} \\ i_{a6} \end{bmatrix} = \bar{J} \times \begin{bmatrix} a_1 \\ a_2 \\ a_3 \\ a_4 \\ a_5 \\ a_6 \end{bmatrix} + \bar{B} \begin{bmatrix} \omega_1 \\ \omega_2 \\ \omega_3 \\ \omega_4 \\ \omega_5 \\ \omega_6 \end{bmatrix} \quad (4.12)$$

Using the above equation, two mechanical parameters of the system are calculated.

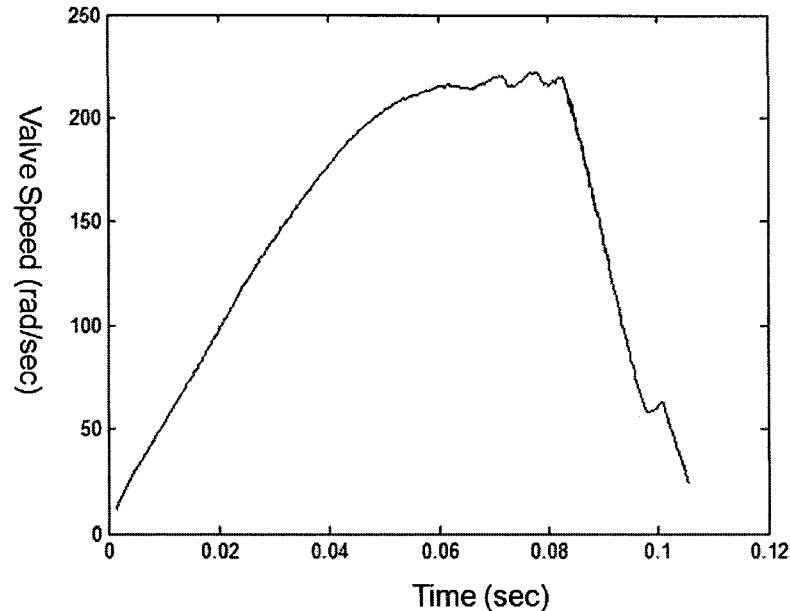


Fig. 4.4 Plate speed response for the applied 10 V

As can be seen in the Fig. 4.4 after 0.08 seconds the system speed drops suddenly to zero, which shows the valve is blocked at this time. This is also observable from the current response of the system when the same voltage of 10 V is applied to the system, Fig. 4.5. As can be seen, immediately after the current reaches the steady state value of 1.06Amp, there is a sudden jump to 7.4 Amp, and then it reaches another steady condition. The reason for this jump is that after almost 0.08 seconds the plates reach the block, the EGR valve in this experiment can only open 90°, cannot go further. So, only the data within the 0.08 seconds, prior to the time plates hit the block, is valid to model the system.

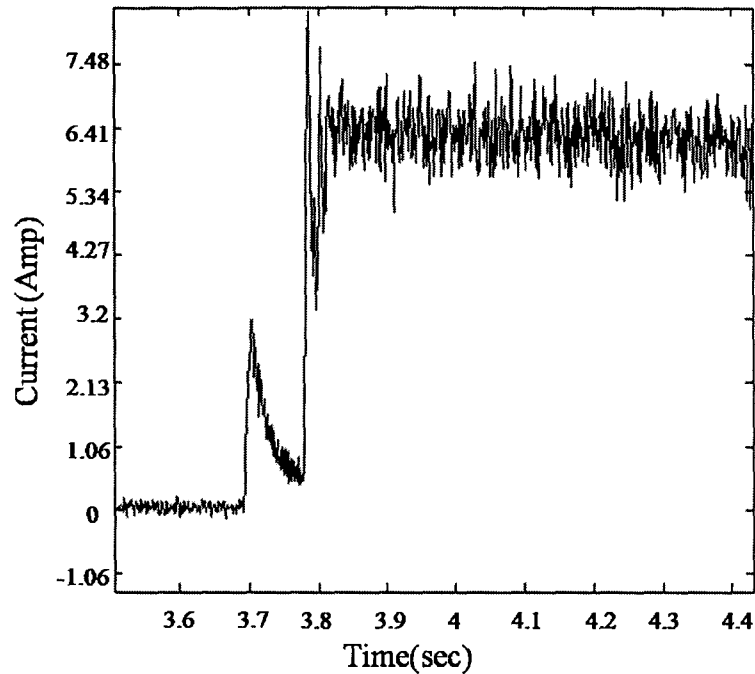


Fig. 4.5 Plate current response for the applied 10 V

Each experiment is repeated 2-3 times and the average taken to get more accurate values.

4.2 Validation of Model Parameters

Through more investigation by evaluating the identified parameters with a Simulink model, it was found that the system viscous damping factor identified through experimentation, slightly changes when the applied voltage varies between 0 to 10 V. This slight difference can be due to the nonlinearity of the system. So in the open loop experiment, the full operating range is treated as a series of narrow operating range problems and 2 different linear models, each valid for a range of operation, is developed. However, in the close loop experiment, when there is the feedback in the loop this model

uncertainty is compensated and only the first set of parameters is accurate enough to show the system model.

Table 4.1 shows the identified parameters for two operating ranges:

Table 4.1. EGR valve identified parameters

System Parameters	0 - 5 v range	5 – 10 v range
$\bar{J}(kgm^{-1})$	2.94×10^{-4}	2.94×10^{-4}
$\bar{B}(Nm/rad/s)$	0.0199	0.0075
$R_a(\Omega)$	3	3
$L_a(H)$	0.0012	0.0012
$K_t(Nm / A)$	0.019	0.019
n	0.057	0.057

The model obtained in this section is used in both control algorithm and in observers model used to estimate the spring torque.

CHAPTER 5

Control Design for EGR Valve and Experimental

Validation

5.1 GPC Algorithm for Control of the EGR Valve

In order to control the EGR valve using the GPC algorithm, the input and output of the system are allowed to be $U(t)$ and $\theta(t)$. In the close loop system when there is a feedback in the system, the uncertainty in the viscous damping factor of the valve is compensated. So only the first set of model parameters identified in Chapter 4 is accurate enough to use in the GPC algorithm.

Since in the GPC method the transfer function of the system is used, the EGR valve is modeled as:

$$\frac{y(t)}{u(t)} = \frac{\theta(t)}{U(t)} = \frac{0.3295}{3.5282 \times 10^{-7} s^3 + 9.0594 \times 10^{-4} s^2 + 0.1683s} \quad (5.1)$$

A and B polynomials in equation (2.1) can be obtained when the transfer function of the system is transferred to the Z domain:

$$A(z^{-1}) = 1 - 1.91z^{-1} + 0.988z^{-2} - 0.07671z^{-3}$$

$$B(z^{-1}) = 2.48 \times 10^{-5} + 1.818 \times 10^{-4} z^{-1} + 1.119 \times 10^{-4} z^{-2} + 5.414 \times 10^{-6} z^{-3}$$

Via applying equation $\tilde{A}(z^{-1}) = \Delta A(z^{-1})$, the plant model is used to obtain the $\tilde{A}(z^{-1})$ equation:

$$\tilde{A}(z^{-1}) = \Delta A(z^{-1}) = 1 - 2.91z^{-1} + 2.898z^{-2} - 1.0647z^{-3} + 0.07671z^{-4}$$

In order to calculate the future outputs of the plant, the two Controller Auto Regressive Integrated Moving Average and Diophantine equations are used. When $\tilde{A}(z^{-1})$ is calculated the E_j and F_j polynomials in equation (2.5) for a 4 control horizon are obtained by dividing 1 over the $\tilde{A}(z^{-1})$ to the point that the remainder can be factorized as $z^{-j}F_j(z^{-1})$. So these polynomials are calculated as:

$$E_1 = 1$$

$$E_2 = 1 + 2.91z^{-1}$$

$$E_3 = 1 + 2.91z^{-1} + 5.5701z^{-2}$$

$$E_4 = 1 + 2.91z^{-1} + 5.5701z^{-2} + 8.8405z^{-3}$$

$$F_1 = 2.91 - 2.898z^{-1} + 1.0647z^{-2} - 0.07671z^{-3}$$

$$F_2 = 5.5701 - 7.3685z^{-1} + 3.0216z^{-2} - 0.2232z^{-3}$$

$$F_3 = 8.8405 - 13.1205z^{-1} + 5.7073z^{-2} - 0.4273z^{-3}$$

$$F_4 = 12.6054 - 19.9125z^{-1} + 8.9852z^{-2} - 0.6782z^{-3}$$

The future output of the plant is calculated using the following equation:

$$y = Gu + F(z^{-1})y(t) + G'(z^{-1})\Delta u(t-1) \quad (5.2)$$

Notice that the last two terms in equation (5.2) only depend on the past and can be grouped into f leading to:

$$y = Gu + f \quad (5.3)$$

where:

$$y = \begin{bmatrix} \hat{y}(t+1|t) \\ \hat{y}(t+2|t) \\ \hat{y}(t+3|t) \\ \hat{y}(t+4|t) \end{bmatrix} \quad u = \begin{bmatrix} \Delta u(t) \\ \Delta u(t+1) \\ \Delta u(t+2) \\ \Delta u(t+3) \end{bmatrix}$$

$$G(z^{-1}) = E(z^{-1})B(z^{-1}) = \begin{bmatrix} 2.495 \times 10^{-5} & 0 & 0 & 0 \\ 2.5725 \times 10^{-5} & 2.495 \times 10^{-5} & 0 & 0 \\ 7.9566 \times 10^{-4} & 2.5725 \times 10^{-5} & 2.495 \times 10^{-5} & 0 \\ 1.5 \times 10^{-3} & 7.9566 \times 10^{-4} & 2.5725 \times 10^{-5} & 2.495 \times 10^{-5} \end{bmatrix}$$

$$f = \begin{bmatrix} 1.84 \times 10^{-4} \Delta u(t-1) + 1.14 \times 10^{-4} \Delta u(t-2) + 5.541 \times 10^{-6} \Delta u(t-3) \\ + 2.936y(t) - 2.951y(t-1) + 1.0939y(t-2) - 0.07891y(t-3) \\ 6.5422 \times 10^{-4} \Delta u(t-1) + 3.4024 \times 10^{-4} \Delta u(t-2) + 1.6268 \times 10^{-5} \Delta u(t-3) \\ + 5.6691y(t) - 7.5702y(t-1) + 3.1328y(t-2) - 0.2317y(t-3) \\ 1.3 \times 10^{-3} \Delta u(t-1) + 6.6255 \times 10^{-4} \Delta u(t-2) + 3.1412 \times 10^{-5} \Delta u(t-3) \\ + 9.0743y(t) - 13.5967y(t-1) + 5.9697y(t-2) - 0.4473y(t-3) \\ 2.4 \times 10^{-3} \Delta u(t-1) + 1.03 \times 10^{-3} \Delta u(t-2) + 5.0281 \times 10^{-5} \Delta u(t-3) \\ + 13.0454y(t) - 20.8086y(t-1) + 9.4791y(t-2) - 0.7181y(t-3) \end{bmatrix}$$

Now that the future outputs of the plant are obtained, the objective function J can be calculated:

$$J = \frac{1}{2} u^T H u + b^T u + f_0 s \quad (5.4)$$

where:

$$H = 2(\delta G^T G + \lambda I)$$

$$b^T = 2\delta(f - w)^T G$$

$$f_0 = \delta(f - w)^T (f - w)$$

By making the gradient of J equal to zero, the minimum of J is obtained:

$$u = -H^{-1} b = (\delta G^T G + \lambda I)^{-1} \delta G^T (w - f) \quad (5.5)$$

The control signal sent to the plant is the first element of the vector u which is given by:

$$\Delta u(t) = K(w - f) \quad (5.6)$$

Where K is the first row of matrix $(\delta G^T G + \lambda I)^{-1} \delta G^T$ and w is the defined reference trajectory.

It is observed that the set of weights $\lambda(j) = 1 \times 10^{-6}$ and $\delta(j) = 35$ gives the best performance.

The reference trajectory is defined as a smooth approximation from the current value of the output towards the known reference by means of the first order system:

$$w(t) = y(t) \quad w(t+k) = \alpha w(t+k-1) + (1-\alpha)r(t+k) \quad k = 1 \dots N \quad (5.7)$$

α is a parameter between 0 and 1. This parameter is chosen as 0.3 in this case to give a smoother approximation of the real reference.

After all the calculations the matrix K and the control input of the EGR valve is calculated as:

$$K = [88.2 \quad 725.8 \quad 938.3 \quad -22.5]$$

$$\begin{aligned} \Delta u(t) = & 88.2w(t+1) + 725.8w(t+2) + 938.3w(t+3) - 22.5w(t+4) \\ & - 1.7078\Delta u(t-1) - 0.8268\Delta u(t-2) - 0.0392\Delta u(t-3) \\ & - 1.2594 \times 10^4 y(t) + 1.8044 \times 10^4 y(t-1) - 7.7584 \times 10^3 y(t-2) + 578.7171y(t-3) \end{aligned} \quad (5.8)$$

The final block diagram of the EGR valve controlled by the GPC controller is shown in Fig. 5.1:

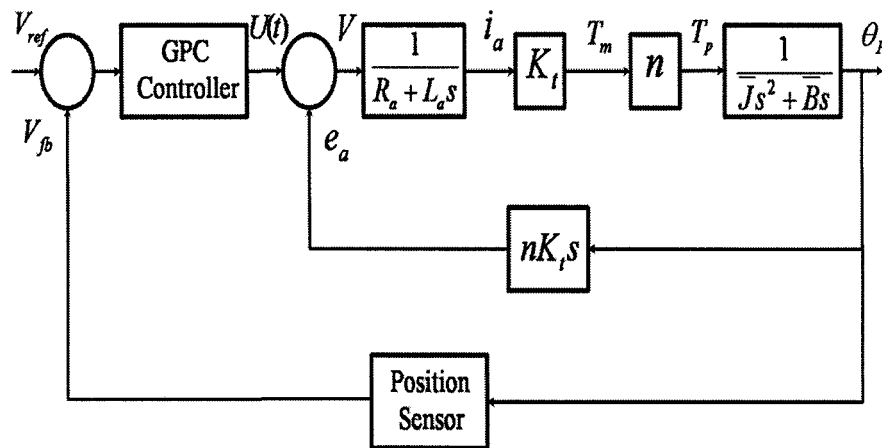


Fig. 5.1 The block diagram of the EGR valve controlled by GPC

The input of the system is a voltage applied from the Opal-RT output. The GPC controller uses the model of the system to predict the future output of the system while minimizing

the system error. Plate position is the output of the system which converts to a DC voltage by the position sensor. This signal is fed back to update the controller with new data on position of the valve.

5.2 Experimental Validation

The experimental results for the bi-directional control of the EGR valve are shown in the first part of this section. The performance of GPC method for controlling the EGR valve is shown for different reference voltages. The valve is controlled according to the plate angular position, so in all the results the reference voltage applied to the valve is converted to the plate angular position. Since the spring applies an additional force in closing direction of the plates, the valve response in this direction is faster than the opening condition. Here the model obtained in the model identification part is used. The GPC algorithm in the first experiment is implemented by the DSP with the sampling time of *25 ns*.

Fig. 5.2 illustrates the control result for the case when the valve is currently 27.77 degrees open and a reference position of 83.32 degrees is applied to the system. As can be seen in the magnified figure, Fig. 5.3, plate can be positioned in about 0.5 seconds.

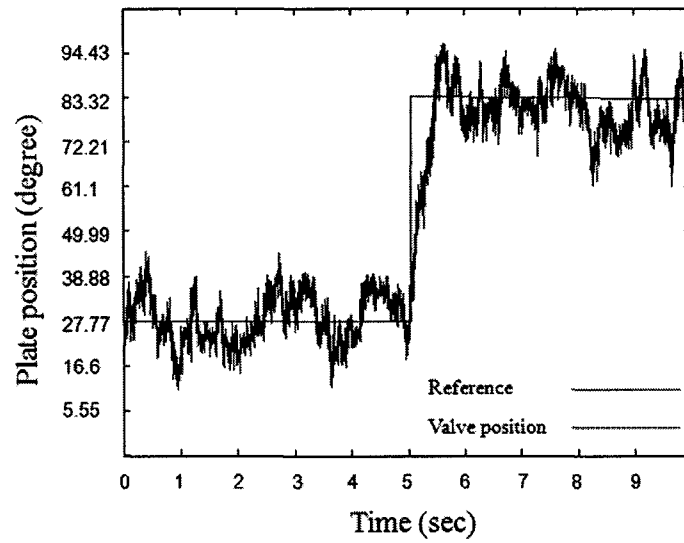


Fig. 5.2 EGR valve response for an 83.32 ° opening reference

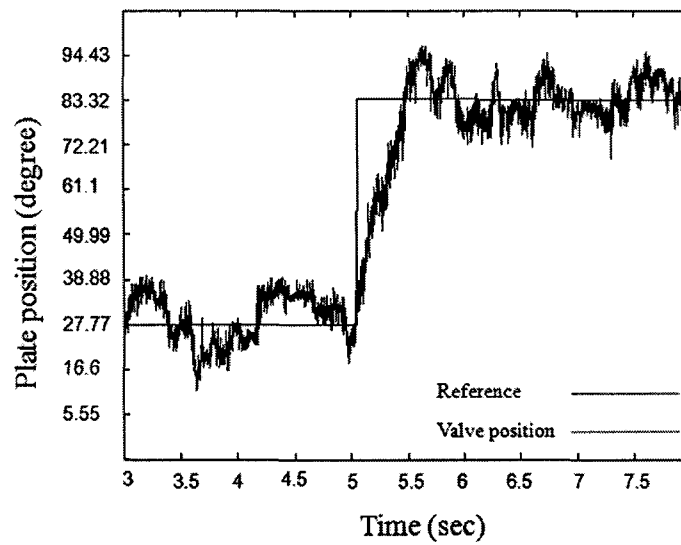


Fig. 5.3 Magnified view of EGR valve response for an 83.32 ° opening reference

The magnified figure for closing direction, Fig. 5.5 , shows that the valve can position in slightly more than 0.2 seconds from the 83.32 degrees open condition to 27.77 degrees.

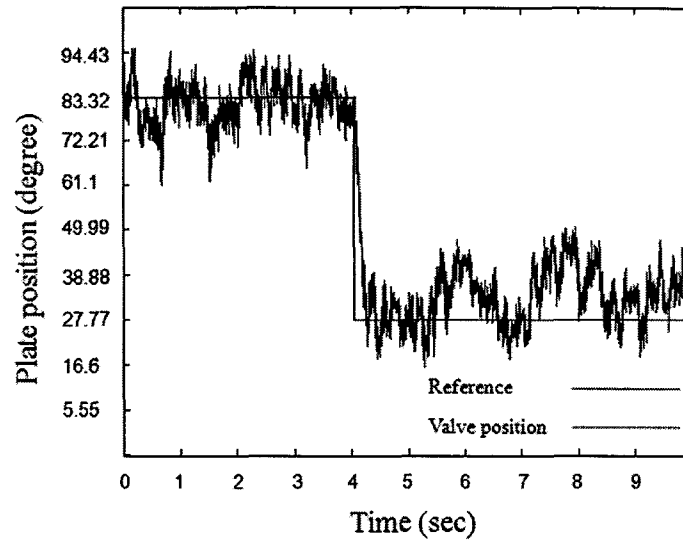


Fig. 5.4 EGR valve response for a 27.77° closing reference

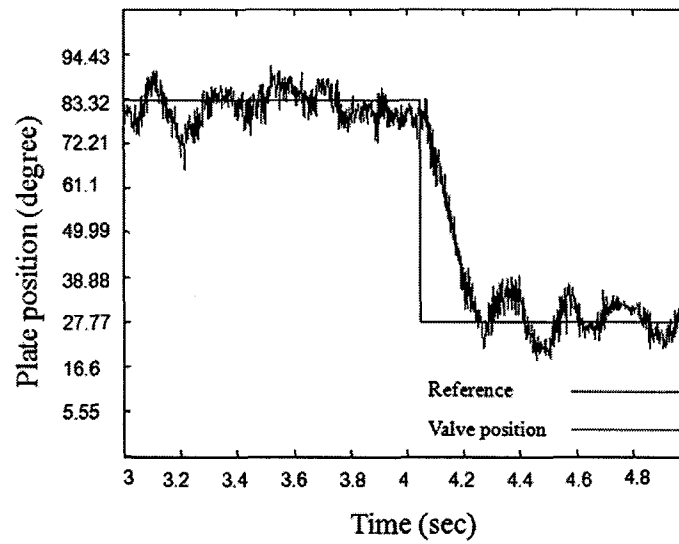


Fig. 5.5 Magnified view of EGR valve response for a 27.77° closing reference

Fig. 5.6 and Fig. 5.7 compare the result of the GPC controller with a PID controller. It can be seen that the GPC controller gives a faster response than the PID controller in both directions.

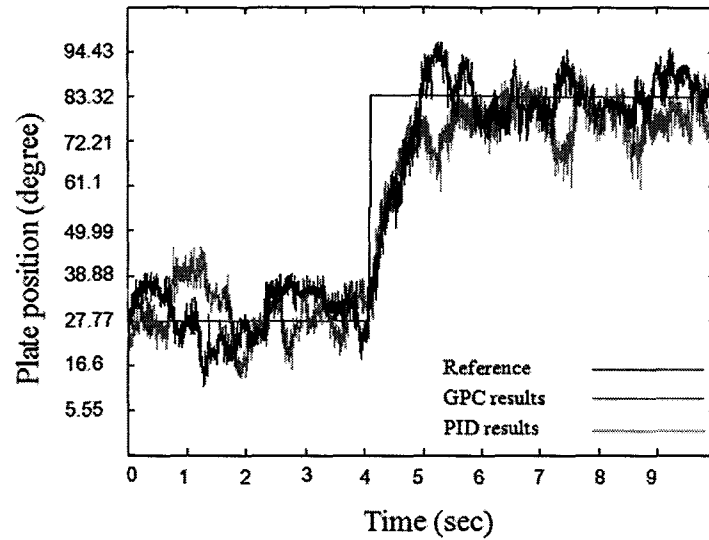


Fig. 5.6 Comparison of the responses of GPC and PID controller in opening direction

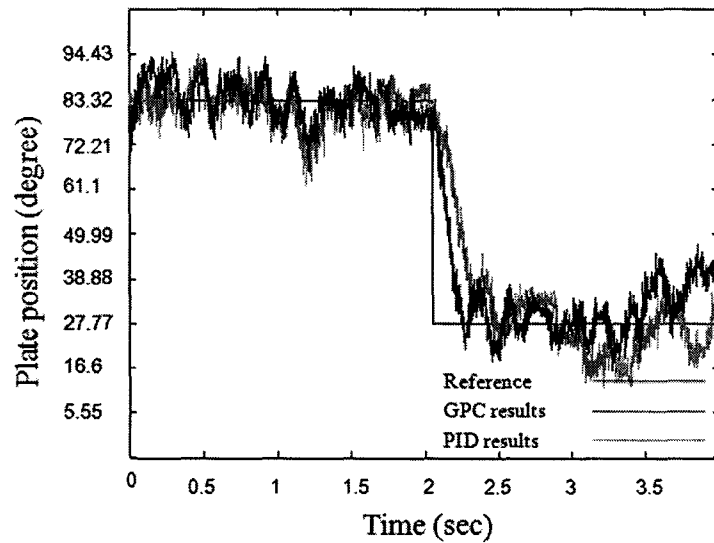


Fig. 5.7 Comparison of the responses of GPC and PID controller in closing direction

Fig. 5.8 shows the control result for the case when a variable reference, sine reference, is applied to the valve. As can be seen the valve is positioned accurately according to the reference voltage.

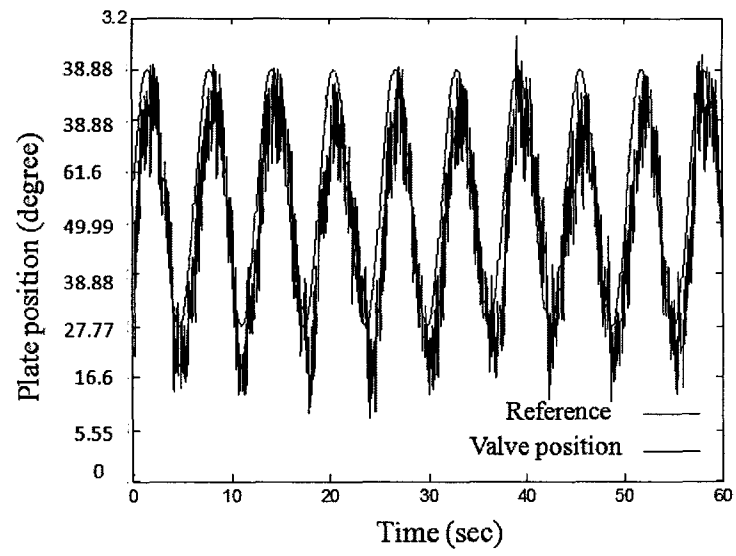


Fig. 5.8 EGR valve response for a sine reference

CHAPTER 6

Estimation of Spring Torque

6.1 Spring Torque Estimation for EGR Valve

The observer for the EGR valve model is designed by considering the state space model of system.

- *Observer Design*

The required variable to be estimated is the spring torque which is treated as a disturbance torque acting on the motor shaft, and a law which relates it with the state variables is used:

$$\hat{T}_{disturbance} = \bar{J} \frac{d\hat{\omega}_p}{dt} + \bar{B}\hat{\omega}_p - K_t i_a \quad (6.1)$$

In this case the estimated disturbance torque includes all the external disturbances including the spring torque. So the spring torque should be calculated out. For this purpose, the dynamometer inertia and viscous damping factor should be added in the above model:

$$\hat{T}_s = (\bar{J} - J_{dyno}) \frac{d\hat{\omega}_p}{dt} + (\bar{B} - B_{dyno})\hat{\omega}_p - K_t i_a \quad (6.2)$$

Since, in this case the dynamometer parameters are unknown, the spring torque is calculated by subtracting the data obtained in the two estimations: with and without the

spring. The disturbance torque for the case with spring is in fact the sum of spring torque and the dynamometer disturbances, equation (6.3), and when the spring is disconnected there is only the dynamometer torque, equation (6.4). In order to calculate the spring torque the data from these two experiments are subtracted and the result is considered as the spring torque (6.5):

$$T_{disturbances}(ws) = T_s + T_{dyno} \quad (6.3)$$

$$T_{disturbances}(wos) = T_{dyno} \quad (6.4)$$

$$T_s = T_{disturbances}(ws) - T_{disturbances}(wos) \quad (6.5)$$

In order to estimate the spring torque, two state variables, motor armature current and plate speed, are considered in the filter model. Even though the filter gives the estimation of the current, the motor armature current is measured in practice and will be used to calculate the estimation of the spring torque. Note that all three filters carry the same model structure and the only difference among them is the filter gain.

The observer model is a replica of system model with faster dynamics. The following table shows the state space model of a general system and its observer:

Table 6.1 State space model of a general system and its observer

System Model (excluding the external disturbances)	Observer Model
$\dot{x} = Ax + Bu$	$\dot{\hat{x}} = A\hat{x} + L(\hat{y} - y) + Bu$
$z = C_1x$	$\hat{z} = C_1\hat{x}$
$y = C_2x$	$\hat{y} = C_2\hat{x}$

where $\hat{x} = \begin{bmatrix} \hat{x}_1 \\ \hat{x}_2 \end{bmatrix} = \begin{bmatrix} \hat{i}_a \\ \hat{\omega}_p \end{bmatrix}$ are the estimation of state variables, \hat{z} is the desired output, \hat{y}

is measured output, and L is the filter gain.

The observer model used to estimate the spring torque is shown in Fig. 6.1:

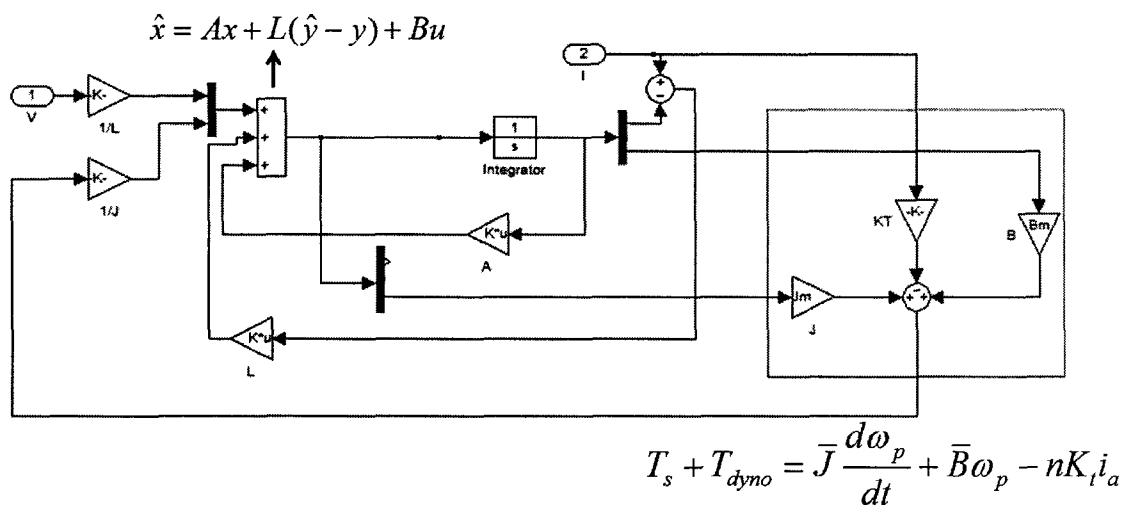


Fig. 6.1 Observer model for spring torque estimation

Here the disturbance torque is estimated and fed back to updates model dynamics. This feedback loop updates the system states considering the last obtained disturbance torque estimate. Without this loop, the model does not consider the effect of disturbance torque

on the state variables. The filter gain is designed by different methods depending on the type of filters used to for the estimation.

1. Kalman Filter

This filter is used when the system is subjected to white noise which originates from the commutator, vibration, Pulse Width Modulated (PWM) control signals, etc. The system model used to design the Kalman filter is given in equation (2.13):

$$\begin{bmatrix} \dot{i}_a \\ \dot{\omega} \end{bmatrix} = \begin{bmatrix} \frac{-R_a}{L_a} & \frac{-nK_e}{L_a} \\ \frac{K_t}{J} & \frac{-B}{J} \end{bmatrix} \begin{bmatrix} i_a \\ \omega \end{bmatrix} + \begin{bmatrix} -\frac{1}{L_a} \\ 0 \end{bmatrix} u + B_0 w_0 \quad (6.6)$$

$$z = \begin{bmatrix} 1 & 0 \\ 0 & 1 \end{bmatrix} \begin{bmatrix} i_a \\ \omega \end{bmatrix} \quad (6.7)$$

$$y = \begin{bmatrix} 1 & 0 \end{bmatrix} \begin{bmatrix} i_a \\ \omega \end{bmatrix} + D_{20} w_0 \quad (6.8)$$

The last two terms in equation (6.6) and (6.8) show the system and measurement noises. The weight D_{20} is set by measuring the covariance of measurement noise. The process noise covariance is relatively difficult to measure. The motor is subjected to un-modeled disturbances; hence the sensor output is more reliable than the process model. Thus it is chosen to be larger measurement noise and tuned by trial and error methods. The Kalman filter gain is then computed using equation (2.15).

2. H_∞ Filter

The system model used to design an H_∞ is:

$$\begin{bmatrix} \dot{i}_a \\ \dot{\omega} \end{bmatrix} = \begin{bmatrix} \frac{-R_a}{L_a} & \frac{-nK_e}{L_a} \\ \frac{K_t}{J} & \frac{-B}{J} \end{bmatrix} \begin{bmatrix} i_a \\ \omega \end{bmatrix} + \begin{bmatrix} -\frac{1}{L_a} \\ 0 \end{bmatrix} u + \begin{bmatrix} -\frac{1}{L_a}w_1 & 0 \\ 0 & -\frac{1}{J}w_2 \end{bmatrix} w \quad (6.9)$$

$$z = \begin{bmatrix} 1 & 0 \\ 0 & 1 \end{bmatrix} \begin{bmatrix} i_a \\ \omega \end{bmatrix} \quad (6.10)$$

$$y = \begin{bmatrix} 1 & 0 \end{bmatrix} \begin{bmatrix} i_a \\ \omega \end{bmatrix} \quad (6.11)$$

It is noted that the accurate value of the motor armature resistance is very hard to obtain in practice. Besides, this resistance could also vary during the life time of motor operation due to the friction erosion between the brush and the commutator. Therefore, such a parameter uncertainty should be considered and is modeled as $R_a + \Delta R_a$.

The disturbance vector, w is taken as $\begin{bmatrix} \Delta R_a \\ T_s \end{bmatrix}$. T_s is considered as one of the uncertainties.

The weights w_1 and w_2 could be added to provide appropriate penalty on the particular uncertainty signals. The filter gain is then calculated using equation (2.18).

3. H_∞ Gaussian Filter

The motor model for designing the H_∞ Gaussian filter is built by combining the Kalman and H_∞ filter models.

$$\begin{bmatrix} \dot{i}_a \\ \dot{\omega} \end{bmatrix} = \begin{bmatrix} \frac{-R_a}{L_a} & \frac{-nK_e}{L_a} \\ \frac{K_t}{J} & \frac{-B}{J} \end{bmatrix} \begin{bmatrix} i_a \\ \omega \end{bmatrix} + \begin{bmatrix} \frac{1}{L_a} \\ 0 \end{bmatrix} u + B_0 w_0 + \begin{bmatrix} -\frac{1}{L_a} w_1 & 0 \\ 0 & -\frac{1}{J} w_2 \end{bmatrix} w \quad (6.12)$$

$$z = \begin{bmatrix} 1 & 0 \\ 0 & 1 \end{bmatrix} \begin{bmatrix} i_a \\ \omega \end{bmatrix} \quad (6.13)$$

$$y = [1 \quad 0] \begin{bmatrix} i_a \\ \omega \end{bmatrix} + D_{20} w_0 \quad (6.14)$$

The H_∞ Gaussian filter gain is calculated using equation (2.22).

When the inertia of the system is very low indicating very fast system dynamics, it is seen that a higher value of γ is required for stable solutions to equations (2.20) and (2.21).

6.2 Experimental Validation

The Hardware-in-Loop (HIL) results for spring torque estimation in the EGR valve is shown here. The performance of Kalman filter, H-Infinity and H-Infinity Gaussian filters are compared with the torque signal obtained from the experiment. The calculated gains are almost the same for the Kalman and H-Infinity Gaussian filter, so their results are so close to each other that the difference cannot be distinguished unless the figure is

magnified about 20 times. Here the model obtained in the model identification part is used.

The figures are plot for the opening period of the valve when the voltage is applied. Since the plate hits the block when it opens about 90 degrees, only the data during this period is valid to use in estimation.

Case 1: Spring torque estimation with nominal parameters identified in Chapter 4 used for observer design

The spring torque estimation result is shown in Fig. 6.2 and its estimated error is shown in Fig. 6.3. Here, the weights used in the uncertainty matrix are $w_1 = 1$ and $w_2 = 0.1$. The value of the resistor is $R = 3\Omega$ and the weighting factor in the H_∞ and H_∞ Gaussian filter is chosen as $\gamma = 5.01$.

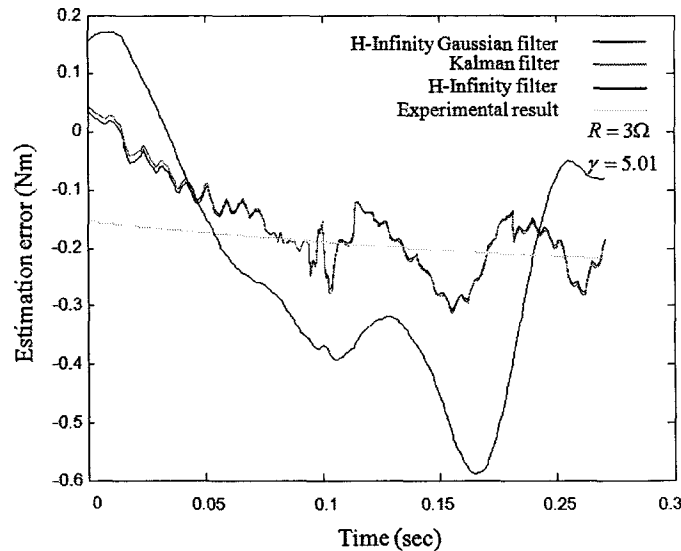


Fig. 6.2 Estimated spring torque result, Case 1

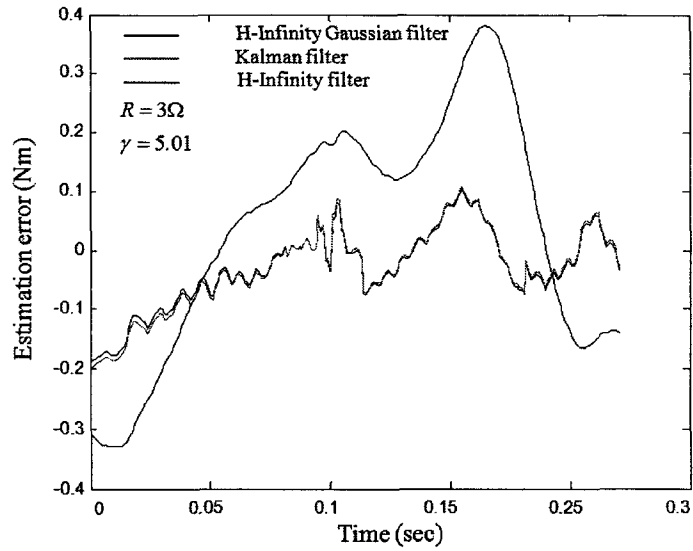


Fig. 6.3 Spring torque estimation error, Case 1

Case 2: Spring torque estimation with nominal parameters identified in Chapter 4 used for observer design when $\gamma = 99.8$.

When the value of γ is increased the H_∞ Gaussian and H_∞ filter gains slightly change. So there is only a very small difference in the estimation result. Fig. 6.4 shows the estimation result for this case and Fig. 6.5 shows its error.

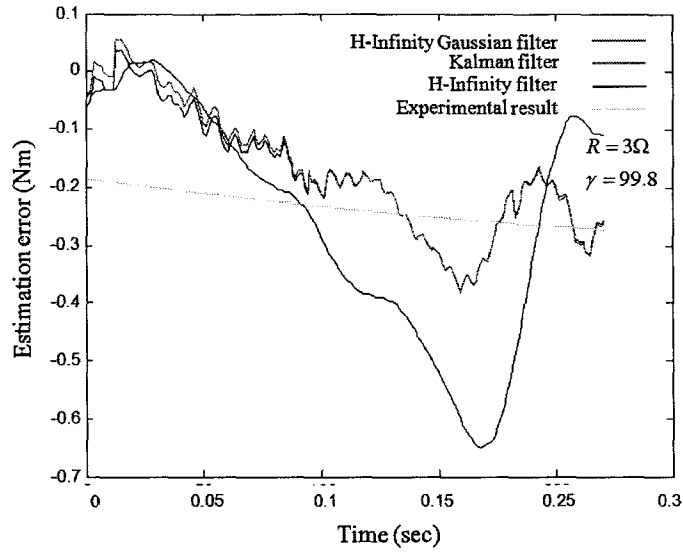


Fig. 6.4 Estimated spring torque, Case 2

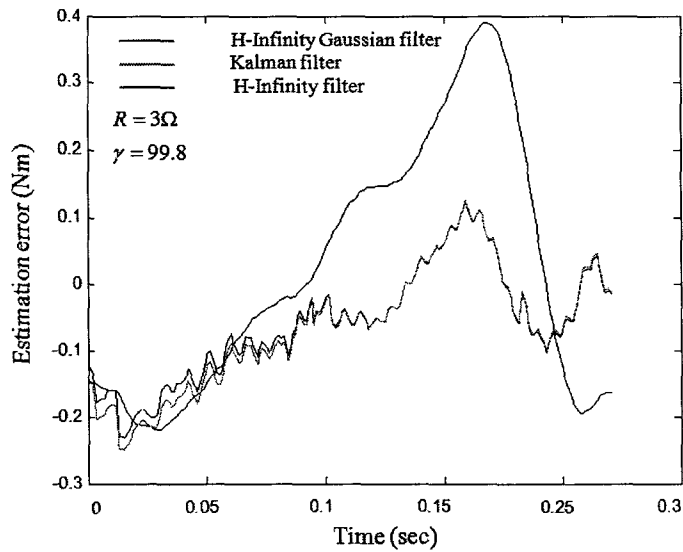


Fig. 6.5 Spring torque estimation error, Case 2

Case 3: Spring torque estimation with nominal parameters identified in Chapter 4 used for observer design with 33% parameter uncertainty in motor resistance.

Fig. 6.6 and Fig. 6.7 show the estimation of spring torque and estimation error when there is a 33% decrease in motor resistance value from its nominal value.

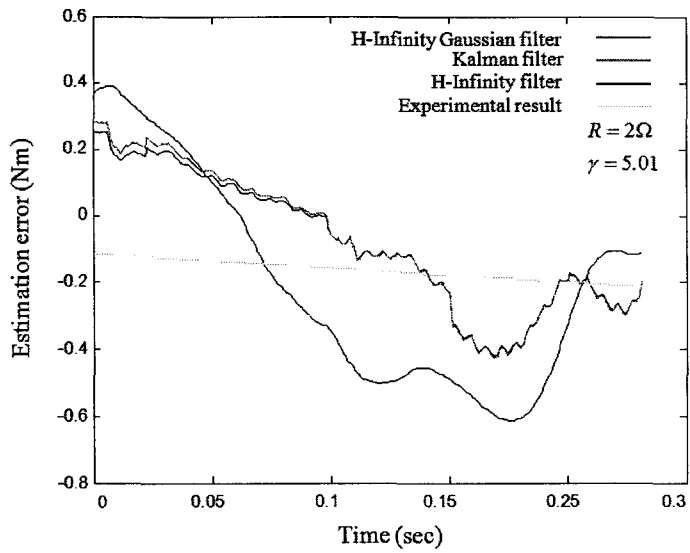


Fig. 6.6 Estimated spring torque , Case 3

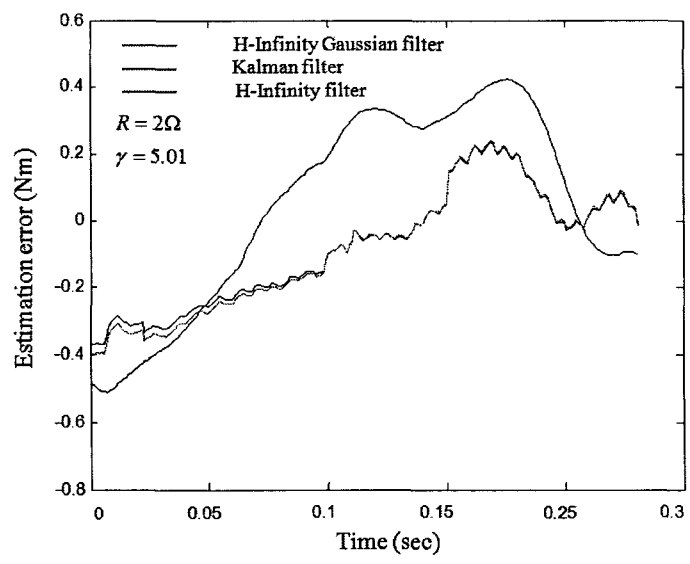


Fig. 6.7 Spring torque estimation error, Case 3

CHAPTER 7

7.1 Conclusion

The significant effect of the EGR system on reducing the engine emissions makes this system an important control target. To control the Nox emission more accurately, the EGR valve should be controlled precisely in both opening and closing directions. So a fast and accurate method is necessary to meet the required performance. Since the Generalized Predictive Control method uses the model of the system to predict the future output of the system while minimizing the system error, it can potentially provide a faster response while the accuracy can be improved during the operating process in the long-run.

The GPC method uses the model of the system to predict the future output of the system while minimizing the system error to obtain the control input. So, in the first step of this work both the state space model and transfer function of the EGR valve are derived, and the system parameters are identified. Then, the GPC algorithm is applied to the plant. The experimental results obtained by implementing this method to the EGR valve which is modeled in the first part prove a fast and accurate position control of the valve in both directions and with both constant and variable references.

In advanced engine control a better control on EGR valve is obtained if the total effective torque on the plate is known and considered in the control loop. Besides the motor torque which is provided by the controller, there is also the spring torque acting on the plate shaft. The purpose of the second part of this work is to estimate this spring torque which

is a step to a more accurate valve and consequently engine control. So based on the work done in the first part the spring torque is considered as a disturbance torque on the plate shaft and three robust filters, Kalman, H_∞ and H_∞ Gaussian, are used to estimate its value. The significance of these three filter designs and their performance under different disturbance conditions are also studied. For a system with uncertain model parameters an H_∞ or H_∞ Gaussian filter is required. The Kalman filter is recommended when the model of the good performance towards white noise is the requirement. Although the time period to run the experiment and estimate the spring torque is too short the HIL experimental results using these three filters show a good estimate of spring torque.

7.2 Future Work

As the next step of this work the performance of the EGR valve controlled by the Generalized Predictive Controller can be validated when the EGR valve is mounted on a real engine setup when there is the exhaust gas flowing through the valve. Since this method uses the model of the system, if the parameters of the valve and motor are known a better control algorithm could be achieved for the system.

Also, in order to have a faster and more accurate control of the valve, the spring torque signal estimated by the observers could be used in the control loop. This signal should be considered as one of the torque factors acting on the motor shaft. A systematic method to determine the set of weights on the uncertainties should be investigated to obtain the best performance of the filter. When arbitrarily chosen weights are used by trial and error method, the best performance of filter is not guaranteed.

References

1. Zheng, M., Reader, G. T., and Hawley, J. G., "Diesel Engine Exhaust Gas Recirculation—a Review on Advanced and Novel Concept," *Energy Conversion and Management*. 45(6):883–900, 2004.
2. Zheng, M., Kumar, R., and Reader, G. T., "Adaptive Fuel Injection Tests to Extend EGR Limits on Diesel Engines," SAE Technical Paper 013426, 2006.
3. Ladommatos, N., Abdelhalim, S. M., Zhao, H., and Hu, Z., "The Dilution, Chemical, and Thermal Effects of Exhaust Gas Recirculation on Diesel Engine Emissions—Part 1: Effect of Reducing Inlet Charge Oxygen," SAE Technical Paper 961165, 1996.
4. Ladommatos, N., Abdelhalim, S. M., Zhao, H., and Hu, Z., "The Dilution, Chemical, and Thermal Effects of Exhaust Gas Recirculation on Diesel Engine Emissions—Part 2: Effects of Carbon Dioxide," SAE Technical Paper 961167, 1996.
5. Itoyoma, H., Uchida, M., and Miwa, H., "A Study of an Egr Control System for Diesel Engines Based on an Intake/Exhaust System Model," SAE Technical Paper 970621, 1997.
6. Yamada, T., Kondoh, N., Ikeya, N., and Salto, A., "New Egr System for Heavy-Duty Diesel Engines," SAE Technical Paper 980775, 1998.
7. Baert, R. S. G., Beckman, D. E., and Veen, A., "Efficient EGR Technology for Future HD Diesel," SAE Technical paper 010837, 1999.
8. Abd-Alla, G. H., "Using Exhaust Gas Recirculation in Internal Combustion Engines: a review," *Energy Conversion and Managmt* 43(8): 1027-1042, 2002.
9. Duernholz, M., and Endres, H., "A Measure to Reduce Exhaust Emissions of DI diesel Engines," SAE Trans. Fuel Systems Gen. Emissions 10: 151-158
10. Peng, H., Cui, Y., Shi, L., and Deng, K., "Effects of Exhaust Gas recirculation (EGR) on Combustion and Emissions During Cold Start of Direct Injection (DI) Diesel Engine," *Energy J.* 33(3): 471-479, 2008.
11. Oleksiewicz, R. A., "Exhaust Gas Recirculation Control Apparatus," U.S.Patent 6 014 960, Jan 18, 2000.

12. Chang Yang, C., White, G. R., Henrich, R. S., Wang, Y. Y., Janssen, J. M., and Hatton, R. C., " EGR Valve Position Sensor Control," U.S.Patent 6 467 469 B2, Oct, 22, 2002.
13. Hardman, K., and Bonne, M. A.," Electrical Exhaust Gas Recirculation Valve Control," U.S. Patent 7 124 751 B2, Oct 24, 2006.
14. Gopp, A. Y., and Patel, S., "Exhaust Gas Recirculation Control System," U.S.Patent 5 690 083, Nov 25, 1997.
15. Camacho, E. F., and Bordons, C., "Model Predictive Control," Springer, London, ISBN 3-540-76241-8, 1999.
16. Clarke, D. W., Mohtadi, C., and Tuffs, P. S., "Generalized Predictive Control. Part I. The Basic Algorithm," *Automatica*. 23(2):137-148, 1987.
17. Clarke, D. W., Mohtadi, C., and Tuffs, P. S., "Generalized Predictive Control. Part II. Extensions and Interpretations," *Automatica*. 23(2):149-160, 1987.
18. Naeem, W., Sutton, R., Chudley, J., Dalglish, F. R., and Tetlow, S., "Predictive a genetic algorithm-based model predictive control autopilot design and its implementation in an autonomous underwater vehicle," *Journal of Engineering for the Maritime Environment* 218(3): 175-188, 2004.
19. Low, K. S., Chiun K. Y., and Ling, K. V., "Evaluating Generalized Predictive Control for a Brushless dc Drive," *IEEE Trans. Power Electron.*, 13:1191–1198, 1998.
20. Low, K. S., and Zhuang, H., "Robust Model Predictive Control and Observer for Direct Drive Applications," *IEEE Trans. Power Electron.* 15:1018–1028, 2000.
21. Giuseppe S.Buja, Roberto Menis, Maria In& Valla; "Disturbance Torque Estimation in a Sensorless DC Drive", *IEEE Transaction on Industrial Electronics*, 42, No. 4: 351-357, 1995.
22. Smitha Cholakkal and Xiang Chen, "Fault Tolerant Control of Electric Power Steering Using H-infinity Filter-Simulation Study" *Proc. IEEE IECON Conference*. 1551-1556, 2009.
23. Smitha Cholakkal and Xiang Chen, "Fault Tolerant Control of Electric Power Steering Using Robust Filter-Simulation Study", *IEEE Vehicle Power and Propulsion Conference*. 1244-1249, 2009.

24. Xiang Chen and Kemin Zhou, "H ∞ Gaussian Filters on Infinite Time Horizon", *IEEE Transactions on Circuits and Systems-I: Fundamental Theory and Applications*.49, No.5:674-679, 2002.
25. Nazila Rajaei, Xiaoye Han, Xiang Chen, and Ming Zheng, " Model Predictive Control of Exhaust Gas Recirculation Valve", SAE World Congress. 2010-01- 0240.
26. Baert, R. S. G., Beckman, D. E., and Veen, A., "Efficient EGR Technology for Future HD Diesel," SAE Technical paper 010837, 1999.
27. Abd-Alla, G. H., "Using Exhaust Gas Recirculation in Internal Combustion Engines: a review," *Energy Conversion and Management*, 43(8): 1027-1042, 2002.
28. Dan Simon, "Optimal State Estimation," Wiley – Interscience, 2006.
29. Xiang Chen and Kemin Zhou, "H ∞ Gaussian Filters on Infinite Time Horizon," *IEEE Transactions on circuits and System–I: Fundamental Theory and Applications*, Vol.49, No. 5, 674-679, May 2002.
30. Yaakov Bar-Shalom, Xiao-Rong Li, Thiagalingam Kirubarajan, "Estimation with Applications to Tracking and Navigation", John Wiley & Sons, Inc.,2001.
31. Kemin Zhou and John C. Doyle, *Essentials of Robust Control*, Prentice Hall, New Jersey, 1998.
32. M. Baric, I. Petrovic, N. Peric, "Neural network based sliding mode control of electronic throttle" *Engineering Applications of Artificial Intelligence*, 951-961, 2005.
33. U. Ozguner, S. Hong, and Y. Pan, "Discrete-time Sliding Mode Control of Electric Throttle Valve", proceedings of 40th IEEE Conference on Decision and Control, Orlando, 1819-1824, 2001.
34. C. Rossi, A. Tilli and A. Tonielli, "Robust Control of a Throttle Body for Drive by Wire Operation of Automotive Engine", *IEEE Transaction on Control System Technology*, 993-1002, 2000.
35. Martin Horn, Anton Hofer, and Markus Reichhartinger, "Control of an Electric Throttle Valve Based on Concepts of Sliding-Mode Control" 17th IEEE International Conference on Control Applications, 2008.

Vita Auctoris

Nazila Rajaei was born in Isfahan, Iran in 1985. She received her B.Sc degree in Electrical Engineering from Azad university of Najafabad in 2007. She is currently a candidate for the Master's degree in Electrical and Computer Engineering department at the University of Windsor and plan to graduate in summer 2010.